

# ORIGIN AND GROWTH OF NUCLEAR STAR CLUSTERS AROUND MASSIVE BLACK HOLES

FABIO ANTONINI

Canadian Institute for Theoretical Astrophysics, University of Toronto, 60 St. George Street, Toronto, Ontario M5S 3H8, Canada  
*Draft version November 8, 2018*

## ABSTRACT

The centers of stellar spheroids less luminous than  $\sim 10^{10} L_{\odot}$  are often marked by the presence of nucleated central regions, called “nuclear star clusters” (NSCs). The origin of NSCs is still unclear. Here we investigate the possibility that NSCs originate from the migration and merger of stellar clusters at the center of galaxies where a massive black hole (MBH) may sit. We show that the observed scaling relation between NSC masses and the velocity dispersion of their host spheroids cannot be reconciled with a purely “in-situ” dissipative formation scenario. On the other hand, the observed relation appears to be in agreement with the predictions of the cluster merger model. A dissipationless formation model also reproduces the observed relation between the size of NSCs and their total luminosity,  $R \propto \sqrt{\mathcal{L}_{\text{NSC}}}$ . When a MBH is included at the center of the galaxy, such dependence becomes substantially weaker than the observed correlation, since the size of the NSC is mainly determined by the fixed tidal field of the MBH. We evolve through dynamical friction a population of stellar clusters in a model of a galactic bulge taking into account dynamical dissolution due to two body relaxation, starting from a power-law cluster initial mass function (CIMF) and adopting an initial total mass in stellar clusters consistent with the present-day cluster formation efficiency of the Milky Way (MW). The most massive clusters reach the center of the galaxy and merge to form a compact nucleus; after  $10^{10}$  years, the resulting NSC has properties that are consistent with the observed distribution of stars in the MW NSC. When a MBH is included at the center of a galaxy, globular clusters are tidally disrupted during inspiral, resulting in NSCs with lower densities than those of NSCs forming in galaxies with no MBHs. We suggest this as a possible explanation for the lack of NSCs in galaxies containing MBHs more massive than  $\sim 10^8 M_{\odot}$ . Finally, we investigate the orbital evolution of globular clusters in giant elliptical galaxies which are believed to always host a MBH at their center rather than a NSC. In these systems an additional mechanism can prevent a NSC from forming: the time for globular clusters to reach the center of the galaxy is much longer than the Hubble time.

*Subject headings:* galaxies: Milky Way Galaxy- Nuclear Clusters - stellar dynamics

## 1. INTRODUCTION

Many galaxies, over the whole Hubble sequence, show nucleated central regions often referred to as “nuclear star clusters” (NSCs). These systems are among the densest star clusters observed, with effective radii of a few parsecs and central luminosities up to  $\sim 10^7 L_{\odot}$  (Matthews & Gallagher 1997; Carollo et al. 1997, 1998; Böker et al. 2002; Balcells et al. 2007; Graham & Guzmán 2003; Böker et al. 2004; Côté et al. 2006; Turner et al. 2012). The total frequency of nucleation is as large as 80% for galaxies fainter than  $M_B = -19.5$ , while NSCs tend to disappear in galaxies brighter than this magnitude.

There is no consensus on how NSCs form. A *dissipative* origin bases on the hypothesis of radial gas inflow into the galactic center and requires efficient dissipation mechanisms to work (e.g., Loose et al. 1982). In this model, a NSC consists mostly of stars that formed locally (Schinnerer et al. 2006, 2008; Milosavljević 2004; Emsellem & van de Ven 2008; Shlosman & Begelman 1989; Bekki 2007).

Alternatively, NSCs could have a *dissipationless* origin in which massive stellar (globular-like) clusters migrate to the center due to dynamical friction and

merge to form a dense nucleus growing up to the size of observed NSCs (Tremaine et al. 1975). Observations of NSCs in dE galaxies suggest that the majority of these systems could be the result of accumulating mass in the form of orbitally decayed globular clusters. Numerical studies have also shown that such a formation model is consistent with the measured sizes and luminosities of nuclei (Capuzzo-Dolcetta 1993; Bekki et al. 2004; Capuzzo-Dolcetta & Mocchi 2008; Hartmann et al. 2011). In addition, stellar population synthesis studies of NSC spectra suggest that most of the mass usually resides in stars as old as typical globular clusters ( $\sim 10$  Gyr; Figer et al. 2004; Böker 2010). On the other hand, the observed correlation between colors and luminosities together with the complex star formation histories that often characterize the central region of galaxies, may be difficult to explain on the basis of a dissipationless origin, unless there is some contribution from continuous or recurrent star formation in addition to the ancient globular cluster stars (Antonini et al. 2012). This suggests that dissipation and dissipationless processes are not exclusive, and NSCs might indeed originate from a combination of the two processes.

Due to their small sizes and their crowded stellar fields, galactic nuclei beyond the Local Group are typically unresolved, and the only quantities that can be determined are integrated properties such as half-mass radius and

total luminosity. A radial density profile and velocity structure can be reliably determined only for the Milky Way (MW) NSC (Genzel et al. 2003; Schödel et al. 2007; Graham & Spitler 2009; Oh et al. 2009), which, due to its proximity ( $\sim 8$  kpc), can be resolved into individual stars (Schödel et al. 2007; Schödel et al. 2009). In addition to the MW, NGC 205 also has a spatially-resolved NSC (Figure 2 of Merritt 2009). The MW NSC has an estimated mass of  $\sim 10^7 M_\odot$  (Launhardt et al. 2002; Schödel et al. 2008) and hosts a massive black hole (MBH) whose mass,  $\sim 4.3 \times 10^6 M_\odot$ , is uniquely well determined (Genzel et al. 2003; Ghez et al. 2008; Gillessen 2009). A number of other galaxies also contain both a NSC and a MBH (Seth et al. 2008; Graham & Driver 2007; Graham & Spitler 2009), that have comparable masses. In models of NSCs, the dynamical influence of a MBH should therefore be considered, at least in bulges brighter than about  $10^9 L_\odot$  which are believed to always contain a MBH (Ferrarese & Ford 2005).

More recently, we have presented large-scale  $N$ -body simulations of the inspiral and merger of massive clusters in the inner regions of the Galaxy (Antonini et al. 2012). We showed that current observational constraints are consistent with the hypothesis that a large fraction of the MW NSC mass is in old stars brought in by infalling globular clusters. In this paper, we expand on this previous work and use simple analytical considerations to investigate the possibility that globular clusters can migrate through dynamical friction in the center of galaxies and form compact stellar nuclei. In particular, we focus on how the presence of MBHs at the center of galaxies can impact the merger hypothesis for the formation of their NSC. In order to highlight the role of MBHs in NSC formation, we will systematically present our results for both cases of galaxy with and without central MBH.

This paper is organized as follows. We start in §2 by comparing some of the observed scaling relations for NSCs with the same relations predicted in both the merger and the gas model. In §3 and §4 we develop a simple analytical model for studying the orbital decay of globular clusters in galaxies like the MW, and explore the effect that a central MBH in the galaxy has on the properties of the resulting NSC. In §5 we use an approach similar to that of §3 to follow the orbital evolution of globular clusters near massive MBHs in the central regions of bright elliptical galaxies. In §6 we discuss a variety of astrophysical implications of a dissipationless origin of NSCs and conclude in §7.

## 2. SCALING RELATIONS

The study of NSCs has revealed a number of correlations between their masses and several global properties of their host galaxies, such as velocity dispersion and bulge mass. The existence of such correlations might indicate a direct link among large galactic spacial scales and the much smaller scale of the nuclear environment. While it was for long believed that NSCs and MBHs followed similar scaling relations with their host galaxies (Ferrarese et al. 2006; Wehner & Harris 2006), it is now well established that NCs do not follow any of the scaling relations defined

by MBHs (Balcells et al. 2007; Graham & Spitler 2009; Graham 2012; Scott & Graham 2012; Leigh et al. 2012). Observations also reveal that, unlike globular clusters, NSC half-light radii are luminosity dependent, increasing with increasing total mass (Côté et al. 2006; Forbes et al. 2008). This relation might contain important information on the processes that shaped the central regions of galaxies and their NSCs.

We start here by comparing such observed correlations with predictions from both the dissipative and dissipationless formation models.

### 2.1. $M_{\text{NSC}} - \sigma$ relation

Of the global-to-nucleus relations, the most frequently referred to is the tight correlation between NSC mass,  $M_{\text{NSC}}$ , and the host galaxy's velocity dispersion,  $\sigma$ . Ferrarese et al. (2006) argued that such a correlation has a slope which is consistent with that of the well-known  $M_\bullet - \sigma$  relation obeyed by the MBH mass,  $M_\bullet$ . More recently, a series of papers reached a different conclusion, suggesting that the NSC scaling relations are instead substantially shallower than the corresponding MBH scaling relations (Graham & Spitler 2009; Graham 2012; Scott & Graham 2012; Leigh et al. 2012). The version of the  $M_{\text{NSC}} - \sigma$  relation given in Graham (2012) is

$$\log\left(\frac{M_{\text{NSC}}}{M_\odot}\right) = (6.83 \pm 0.07) + (1.57 \pm 0.24) \log(\sigma/70 \text{ km s}^{-1}). \quad (1)$$

We mention here that the  $M_{\text{NSC}} - \sigma$  relation might be a non-primary correlation, instead resulting from a projection of the fundamental plane, given the observed correlation between  $M_{\text{NSC}}$  and the total host galaxy mass ( $M_{\text{gx}}$ ):  $M_{\text{NSC}} \propto M_{\text{gx}}^{1.18 \pm 0.16}$  (e.g., see Leigh et al. 2012).

#### 2.1.1. Dissipationless model

A predicted  $M_{\text{NSC}} - \sigma$  relation can be easily derived in the globular cluster merger model if we assume that the globular cluster distribution initially follows the stellar light and by using an isothermal sphere density model:  $\rho(r) = \sigma^2/2\pi Gr^2$ , where  $\sigma$  is the 1D velocity dispersion and  $G$  the gravitational constant. The cumulative mass within  $r$  is  $M(r) = rv_c^2/G = 2r\sigma^2/G$ , with  $v_c$  the velocity of a circular orbit. The dynamical friction coefficient for a stellar cluster of mass  $m_{\text{cl}}$  moving in an isothermal sphere model is (Chandrasekhar 1943):

$$\mathbf{f}_{\text{df}} = -4\pi G^2 m_{\text{cl}} \rho(r) \frac{\mathbf{v}}{v^3} \ln \Lambda \left[ \text{erf}(X) - \frac{2X}{\sqrt{\pi}} e^{-X^2} \right], \quad (2)$$

with  $\ln \Lambda$  the Coulomb logarithm and  $X = v/\sqrt{2}\sigma$ . Noting that

$$\frac{1}{r} \frac{dr}{dt} = -|\mathbf{f}_{\text{df}}| \left( \frac{dL}{dr} \right)^{-1}, \quad (3)$$

where  $L (= \sqrt{GM(r)r})$  is the orbital angular momentum, for a cluster moving on a circular orbit we obtain

$$\frac{dr}{dt} = -Gm_{\text{cl}} \ln \Lambda \left[ \text{erf}(X) - \frac{2X}{\sqrt{\pi}} e^{-X^2} \right] / \sqrt{2} r \sigma. \quad (4)$$

Integrating equation (4) yields

$$r_{in} = \left( \sqrt{2} G m_{cl} \ln \Lambda \left[ \operatorname{erf}(X) - \frac{2X}{\sqrt{\pi}} e^{-X^2} \right] t / \sigma \right)^{1/2}. \quad (5)$$

Clusters initially within  $r_{in}$  reach the center at a time  $\leq t$ .

Assuming that the total mass accumulated in the center is equal to the total mass in globular clusters that are initially within  $r_{in}$ , then we obtain (e.g., Tremaine et al. 1975)

$$M_{\text{NSC}} = 2^{5/4} \left( \ln \Lambda \left[ \operatorname{erf}(X) - \frac{2X}{\sqrt{\pi}} e^{-X^2} \right] \langle m_{cl} \rangle t / G \right)^{1/2} \times f \frac{\langle m_{cl} \rangle}{m_{\star}} \sigma^{3/2}, \quad (6)$$

where  $m_{\star}$  is the mass of the field stars,  $\langle m_{cl} \rangle$  is the average globular cluster mass, and  $f$  is the initial number fraction of globular clusters (after galaxy formation) to the total number of stars in the galaxy. Since the term in square brackets in equation (6) is a constant, the globular cluster merger model predicts  $M_{\text{NSC}} \propto \sigma^{3/2}$ .

In the MW, the initial total number of globular clusters,  $N_{cl}(0)$ , can be recovered based on their observed luminosity function and semi-analytical modeling of mass-loss due to stellar evolution and due to tidal interaction with the Galactic environment. Kruijssen & Portegies Zwart (2009) derived a survival fraction of 0.004 for a minimum initial cluster mass  $M_{\text{min}} = 5000 M_{\odot}$ . Assuming 100 present-day globular clusters we have that the total initial number of clusters in the Galaxy is  $10^{4.4}$ . Considering only those GCs that are associated with the bulge on a Hubble time, this gives  $N_{cl}(0) = 10^{3.9}$ , which compared to the total stellar mass of the Bulge,  $\sim 10^{10} M_{\odot}$ , yields  $f \approx 10^{-6}$ . We can rewrite equation (6) as

$$M_{\text{NSC}} = 3 \times 10^7 M_{\odot} \left( \frac{f}{10^{-6}} \right) \left( \frac{\ln \Lambda}{3} \right) \left( \frac{m_{\star}}{M_{\odot}} \right) \left( \frac{\langle m_{cl} \rangle}{10^5 M_{\odot}} \right)^{3/2} \left( \frac{t}{10^{10} \text{yr}} \right)^{1/2} \left( \frac{\sigma}{50 \text{km s}^{-1}} \right)^{3/2}. \quad (7)$$

Despite its simplicity, our model reproduces the observed  $M_{\text{NSC}} - \sigma$  relation both in slope and normalization.

### 2.1.2. Dissipative model

McLaughlin et al. (2006) proposed a NSC in-situ star formation model regulated by momentum feedback. This model is an extension of the argument proposed by King (2003) to explain the  $M_{\bullet} - \sigma$  relation, and invokes the formation of a massive nuclear cluster due to gas inflow and accumulation at the center of the galaxy during the early phases of galaxy evolution. Stellar winds and supernovae from a young nuclear cluster with a standard IMF produce an outflow with momentum flux given by

$$\dot{\Pi} \approx \lambda L_{\text{Edd}} / c = \frac{\lambda 4\pi G M_{\text{NSC}}}{k}, \quad (8)$$

where  $L_{\text{Edd}}$  is the Eddington luminosity calculated by the stellar mass,  $c$  is the speed of light,  $\lambda \sim 0.05$  is related to the mass fraction of massive stars, and

$\kappa \equiv 0.398 \text{cm}^2 \text{g}^{-1}$  is the electron scattering opacity. The outflow is initially momentum conserving and produces an outward force on the gas in the bulge, whose weight is  $W(r) = G M_{\text{gas}}(r) M(r) / r^2$ , with  $M_{\text{gas}}(r)$  the enclosed gas mass and  $M(r)$  the total enclosed mass of the galaxy. For an isothermal potential one finds

$$W = \frac{4f_g}{G} \sigma^4, \quad (9)$$

where  $f_g = 0.16$  is the baryonic mass fraction (Spergel et al. 2003). Requiring that the momentum output produced by the nuclear cluster balances the weight of the gas leads to the relation

$$M_{\text{NSC}} = \frac{f_g \kappa}{\lambda \pi G^2} \sigma^4 = 3 \times 10^7 M_{\odot} \left( \frac{f_g}{0.16} \right) \left( \frac{\lambda}{0.05} \right)^{-1} \left( \frac{\sigma}{50 \text{km s}^{-1}} \right)^4. \quad (10)$$

A similar scaling relation can be derived in protogalaxies with non-isothermal dark matter halos (McQuillin & McLaughlin 2012).

This model is very attractive because it contains no free parameters. In addition, equation (10) is in good agreement with the  $M_{\text{NSC}} - \sigma$  correlation reported by Ferrarese et al. (2006):

$$\log \left( \frac{M_{\text{NSC}}}{M_{\odot}} \right) = (6.91 \pm 0.11) + (4.27 \pm 0.61) \log \left( \frac{\sigma}{54 \text{km s}^{-1}} \right), \quad (11)$$

but, as previously mentioned, it is at odds with Graham (2012) who finds NSC scaling relations considerably shallower than the corresponding MBH scaling relations. The difference between these two studies was due to the proper exclusion of nuclear disks in the sample of Graham (2012) and the larger sample of NSCs used in this latter work. For these reasons we consider the results of Graham more robust and conclude that the McLaughlin et al. model provides a poor description of the observed  $M_{\text{NSC}} - \sigma$  correlation. This suggests that momentum feedback may be not relevant, which would be expected if the NSCs originated elsewhere and were subsequently deposited into their host galaxy centers.

## 2.2. $R - M_{\text{NSC}}$ relation

The size of galactic nuclei clearly correlates with their luminosity, in the sense that brighter NSCs have larger effective radii. The relation is approximately (Côté et al. 2006)

$$R \propto \sqrt{\mathcal{L}_{\text{NSC}}}, \quad (12)$$

where  $R$  is the NSC effective radius (or half-mass radius) and  $L$  its total luminosity. This relation is consistent with the extrapolation of the  $R_{\text{eff}} - \mathcal{L}$  relation for elliptical galaxies.

### 2.2.1. Dissipationless model

In the merger model the radius of the nucleus increases with increasing total mass as globular clusters merge. The brighter, larger mass nuclei are therefore predicted to be spatially very extended. Antonini et al. (2012)

used simple energy arguments to derive the size-mass relation for NSCs in galaxies with no central MBH. For the sake of completeness we repeat this simple calculation in what follows. After a merger the NSC energy,  $E_f = -GM_f^2/2R_f$ , equals the energy of the nucleus before the merger,  $E_i$ , plus the energy brought in by the globular cluster:

$$E_f = E_i + E_o + E_b, \quad (13)$$

with  $E_b$  the internal binding energy of the cluster, and  $E_o \approx -Gm_{\text{cl}}M_i/2R_i$  its orbital energy before the merger.

The equations above permit expressing the mass, energy, and radius of the nucleus recursively as

$$M_{j+1} = (j+1)M_1, \quad (14)$$

$$jE_{j+1} = (j+1)E_j + jE_1, \quad (15)$$

$$(j+1)^2 R_{j+1}^{-1} = j(j+1)R_j^{-1} + R_1^{-1}, j = 1, 2, 3, \dots \quad (16)$$

where the subscript 1 denotes the initial nucleus, and, by assumption,  $M_1 = m$ . Equations (14-16) imply  $R \propto M^{0.5}$  at the time the mass of the nucleus is still comparable to the mass of the infalling clusters. After many mergers the nucleus is much more massive than one globular cluster and the relation steepens to  $R \propto M$ . After 25 mergers, equations (14-16) imply  $R \approx 5R_1$ . The half-mass radii of globular clusters are  $\sim 3$  pc (Jordán et al. 2005), irrespective of their luminosity, so for a nucleus assembled from 25 mergers,  $R \sim 15$  pc. Such a value is in reasonable agreement with the measured half-mass radii for the brightest nuclei. We conclude that a model that attributes the origin of NSCs to the mergers of globular clusters at the centers of galaxies is consistent with the sizes and luminosities of the nuclei.

In a number of galaxies NSCs are observed to co-exist with MBHs. An example of such systems is the MW for which the mass of the NSC,  $M_{\text{NSC}} \sim 10^7 M_\odot$  (Launhardt et al. 2002; Schödel et al. 2008), is somewhat comparable to the mass of the central black hole,  $M_\bullet \sim 4 \times 10^6 M_\odot$  (Ghez et al. 2008; Gillessen 2009). A MBH will disrupt clusters that pass within the radius

$$r_{\text{disr}} \approx 2 \left( \frac{\sigma_{\text{NSC}}}{5\sigma_K} \right)^{2/3} \left( \frac{r_{\text{infl}}}{r_K} \right)^{1/3} r_K, \quad (17)$$

where  $\sigma_K$  is the one-dimensional velocity dispersion of a globular cluster,  $r_K$  its core radius,  $\sigma_{\text{NSC}}$  is the velocity dispersion in the NSC and  $r_{\text{infl}} = GM_\bullet/\sigma_{\text{NSC}}^2$  is the influence radius of the MBH. In the presence of a MBH, the dependence of the half-mass radius  $R$  on  $M_{\text{NSC}}$  is substantially weaker than the observed correlation,  $R \sim M_{\text{NSC}}^{0.2}$  (Antonini et al. 2012), due to the fact that the size of the NSC is determined by the fixed tidal field from the MBH. When a stellar cluster is disrupted, stars that were initially within the cluster core will redistribute locally at a distance  $r_{\text{disr}}$  from the MBH. The density profile of the NSC will therefore have a core of characteristic size  $\sim r_{\text{disr}}$ .

### 2.2.2. Dissipative model

Although the gas model remains somewhat more qualitative there are some indications that the observed  $R - M_{\text{NSC}}$  relation might be difficult to reconcile with a purely dissipative scenario.

Bekki (2007) performed fully self-consistent chemodynamical simulations to investigate how NSCs can form through dissipative gas dynamics. He found that compact nuclei can be formed via dissipative, repeated merger of gaseous (or stellar) clumps that develop from nuclear gaseous spiral arms due to local gravitational instability. These computations showed that fainter NSCs are likely to have a more diffuse configuration due to more negative feedback from SNe II which in turn can prevent NSCs from forming in faint galaxies. The fact that NSC formation is more-strongly suppressed by stronger feedback effects in less-luminous galaxies would explain why brighter dwarf galaxies (dE) are more likely to contain NSCs (van den Bergh 1986). However, simulations also show that more massive NSCs are less extended than their lower mass counterparts, which is the opposite of the observed trend (see Figure 15 of Bekki 2007).

Further investigation of the above inconsistency is needed in order to determine how the results depend on the resolution limit of the simulations and on the adopted initial conditions.

## 3. FORMATION OF NSCS

### 3.1. Phase-space constraints

The above discussion gives some level of reliability to the hypothesis of a dissipationless, merging formation for NSCs. We now wish to test whether the merger of globular clusters can result in a NSC similar to that of the MW. As a first step one can derive the globular cluster parameters required to give a peak density,  $\rho_{\text{NSC}}$ , equal to the observed density of the NSC in the MW, and see whether such parameters are reasonable when compared to typical globular cluster properties<sup>1</sup>.

The stellar cluster central phase space density is given by

$$\frac{\rho_k}{\sigma_K^3} = \frac{9}{4\pi G} \frac{1}{\sigma_K r_K^2}, \quad (18)$$

where  $\rho_K$  is the cluster core density. After inspiral, we require  $\rho_{\text{NSC}}/\sigma_{\text{NSC}}^3 \lesssim \rho_k/\sigma_K^3$ , or

$$\rho_{\text{NSC}} \lesssim \frac{9}{4\pi G} \frac{\sigma_{\text{NSC}}^3}{\sigma_K r_K^2}, \quad (19)$$

so that

$$\begin{aligned} \rho_{\text{NSC}} &\lesssim 1.5 \times 10^7 M_\odot \text{pc}^{-3} \left( \frac{\sigma_{\text{NSC}}}{100 \text{km s}^{-1}} \right)^3 \\ &\times \left( \frac{\sigma_K}{10 \text{km s}^{-1}} \right)^{-1} \left( \frac{r_K}{1 \text{pc}} \right)^{-2}. \end{aligned} \quad (20)$$

The observed NSC density within 0.5 pc at the Galactic Center (GC) is  $\rho_{\text{NSC}} \approx 10^6 M_\odot \text{pc}^{-3}$  (Merritt 2010). Comparing this with equation (20), we obtain

$$\left( \frac{\sigma_K}{10 \text{km s}^{-1}} \right) \left( \frac{r_K}{1 \text{pc}} \right)^2 \lesssim 15. \quad (21)$$

This crude calculation shows that for a MW-like galaxy, the globular cluster parameters required to give the observed peak density of the NSC are quite reasonable.

<sup>1</sup> I am indebted to D. Merritt for suggesting this calculation.

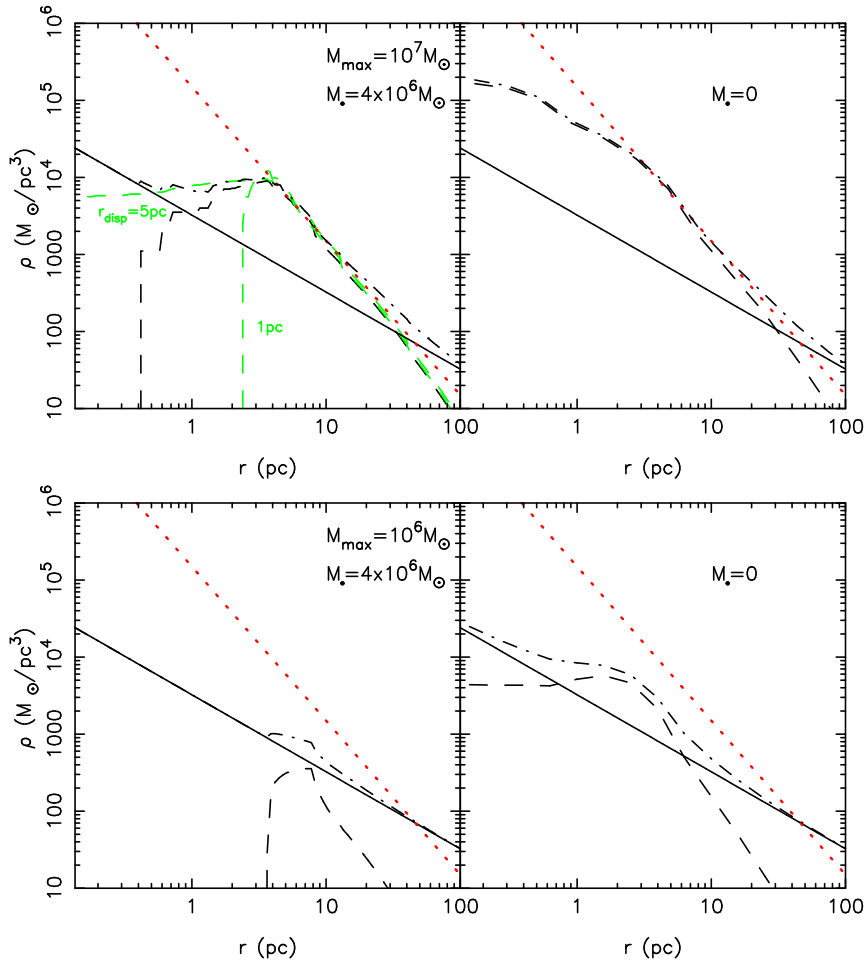


FIG. 1.— Formation of a NSC in a galactic bulge via cluster migration. Dashed and solid lines give respectively the density profiles of the NSC after  $10^{10}$  yr and the density of the background galaxy. Dot-dashed lines are the sum of galaxy and NSC density profiles. Red-dotted lines give the power-law density model  $\rho(r) = 1.5 \times 10^5 M_{\odot} (r/1 \text{ pc})^{-2}$ , representative of the observed radial distribution of stars in the MW NSC (Schödel et al. 2009). We show results assuming that the total mass in stellar clusters is initially 10 per cent of the total galaxy mass and for  $M_{\bullet} = 4 \times 10^6 M_{\odot}$  (left panels), and  $M_{\bullet} = 0$  (right panels). The high mass truncation of the CIMF is  $M_{\text{max}} = 10^7 M_{\odot}$  in the upper panels and  $M_{\text{max}} = 10^6 M_{\odot}$  in the lower panels. Both large values of  $M_{\bullet}$  and small values of  $M_{\text{max}}$  tend to reduce the excess density due to cluster infalls. In making these plots we have assumed the core mass of disrupted clusters is re-distributed after disruption over a region of finite extent  $r_{\text{disp}} = 3 \text{ pc}$ . The green lines in the upper-left panel show results for  $r_{\text{disp}} = 1$  and  $5 \text{ pc}$ . This figure clearly demonstrates how MBHs can control the structure of NSCs forming through globular cluster merging.

### 3.2. NSC formation via cluster migration

A simple analytical model is developed in what follows to evolve a population of stellar clusters subject to migration and dissolution in a galactic bulge and to calculate the influx of migrating clusters into the center of the galaxy. In this way we can address the possibility that a substantial fraction of the NSC mass in galaxies like the MW could have been assembled through cluster migration and mergers.

We assume that the central properties of a stellar cluster (i.e.  $\sigma_K$  and  $r_K$ ) remain unchanged during inspiral and that  $r_t > r_k$ , where  $r_t$  is the cluster tidal (limiting) radius given by (King 1962)

$$r_t = \alpha \frac{\sigma_K}{\sqrt{2}} \left( \frac{3}{r} \frac{d\phi}{dr} - 4\pi G \rho \right)^{-1/2}, \quad (22)$$

with  $\phi$  the galactic potential, and  $\alpha$  a “form factor” that depends on the density distribution within the cluster. For a King model with a large central concentration,  $\alpha \approx 1$ . Equation (22) includes the tidal force due to

the radial gradient in the galaxy potential, the centrifugal force from the cluster’s orbit and assumes that the density of the cluster goes to zero roughly at the radius where the force acting to remove a star is balanced by the attracting force from the rest of the cluster.

The tidal radius of a King model orbiting in a galaxy with a power-law density profile,  $\rho(r) = \rho_0 (r/r_0)^{-\gamma}$ , and containing a MBH at its center, is

$$r_t \approx \frac{\sigma_K}{\sqrt{2}} \left[ 4\pi G \rho_0 \left( \frac{r}{r_0} \right)^{-\gamma} \frac{\gamma}{3-\gamma} + \frac{3GM_{\bullet}}{r^3} \right]^{-1/2}. \quad (23)$$

The radius at which the tidal force from the MBH starts to dominate the tidal force from the stellar cusp (in galaxies containing both) is

$$r = \left( \frac{3(3-\gamma)M_{\bullet}}{\gamma 4\pi \rho_0 r_0^{\gamma}} \right)^{\frac{1}{3-\gamma}}. \quad (24)$$

A King model also satisfies the relation:

$$Gm_t \approx \frac{\sigma_K^2 r_t}{2}, \quad (25)$$

where  $m_t$  is the truncated mass of the globular cluster whose radius is limited by the external tidal field.

Given the cluster central velocity dispersion, equations (23) and (25) can be combined to evaluate, at any radius, the cluster mass permitted by the galaxy tidal field and the mass dispersed along the orbit. This corresponds to a density enhancement with respect to the galactic background of

$$\Delta\rho(r) = \frac{\sigma_K^2}{8\pi Gr^2} \frac{dr_t}{dr}. \quad (26)$$

The resulting radial dependence of the density profile of stars in the growing NSC is easily found to be

$$\Delta\rho(r) \propto \sigma_K^3 \times \begin{cases} \sqrt{\gamma(3-\gamma)} r^{\frac{\gamma-6}{2}} & \text{cusp,} \\ r^{-\frac{3}{2}}/\sqrt{M_\bullet} & \text{black hole.} \end{cases} \quad (27)$$

Steeper density cusps in the distribution of background stars give lower values of the density slope for the resulting NSC. Larger values of  $M_\bullet$  also give smaller densities near the center since the cluster models start being truncated at larger radii and their mass is dispersed over larger spatial scales.

### 3.2.1. Dynamical Friction

We obtain the cluster orbits by using the standard Chandrasekhar's dynamical friction formula (Chandrasekhar 1943) for a self-gravitating cusp (e.g., Merritt et al. 2004; Just et al. 2010):

$$\frac{dr}{dt} = -2 \frac{(3-\gamma)^{3/2}}{4-\gamma} \sqrt{\frac{G}{r_0}} \times \left(\frac{r}{r_0}\right)^{\gamma/2-2} \frac{F(\gamma) \ln \Lambda}{\sqrt{4\pi\rho_0 r_0^3}} m_{\text{cl}}. \quad (28)$$

The coefficient  $F$  is a function of  $\gamma$ , with  $F = (0.193, 0.302, 0.427)$  for  $\gamma = (1, 1.5, 2)$ . We set an initial limiting radius of 40 pc. If  $r_t > 40$  pc (i.e. the model is not truncated), integrating equation (28) yields

$$r(t) = \left[ r_{\text{in}}^{\frac{6-\gamma}{2}} - \frac{(3-\gamma)^{3/2}(6-\gamma)}{(4-\gamma)} \times \sqrt{\frac{G}{4\pi\rho_0}} r_0^{-\gamma/2} F(\gamma) \ln \Lambda m_{\text{cl}} \times t \right]^{\frac{2}{6-\gamma}}, \quad (29)$$

which gives a timescale to reach the center of the galaxy:

$$\tau_\star = 10^{10} \text{ yr} \frac{(4-\gamma)}{(3-\gamma)^{3/2}(6-\gamma)F(\gamma)} \ln \Lambda_3^{-1} \sqrt{\rho_{0,5} r_{0,700}^3} m_{\text{cl},6}^{-1} \left(\frac{r_{\text{in}}}{r_0}\right)^{\frac{6-\gamma}{2}}, \quad (30)$$

with  $\rho_{0,5} = \rho_0/5 M_\odot \text{pc}^{-3}$ ,  $r_{0,700} = r_0/700$  pc,  $\ln \Lambda_3 = \ln \Lambda/3$  and  $m_{\text{cl},6} = m_{\text{cl}}/10^6 M_\odot$ . The coefficient depending on  $\gamma$  is approximately 1.

After a cluster starts being truncated by the galactic tidal field, its mass also becomes a function of radius.

In this case, we computed the cluster orbit by setting  $m_{\text{cl}} = m_t$  in equation (28), obtaining

$$r(t) = \left[ r_{\text{in}}^{3-\gamma} - \frac{(3-\gamma)^3}{(4-\gamma)\sqrt{2\gamma}} \frac{r_0^{-\gamma}}{4\pi G \rho_0} F(\gamma) \ln \Lambda \sigma_K^3 \times t \right]^{\frac{1}{3-\gamma}}. \quad (31)$$

This equation takes into account mass loss due to the interaction with the galactic tidal field, but ignores the possible presence of a MBH<sup>2</sup>. Equation (31) implies that the massive object comes to rest at the center of the stellar system in a time

$$\tau_\star = 3 \times 10^{10} \text{ yr} \frac{(4-\gamma)\sqrt{\gamma}}{(3-\gamma)^3 F(\gamma)} \quad (32)$$

$$\ln \Lambda_3^{-1} \rho_{0,5} r_{0,700}^3 \sigma_{K,10}^{-3} \left(\frac{r_{\text{in}}}{r_0}\right)^{3-\gamma},$$

with  $\sigma_{K,10} = \sigma_K/10$  km s<sup>-1</sup> and the coefficient depending on  $\gamma$  equals to (2.8, 4.27, 9.4) for  $\gamma = (1, 1.5, 2)$ .

These basic formalism assumes that mass loss from the clusters is entirely due to their interaction with the external tidal field and it omits mass loss (evaporation) due to internal dynamics. Since the only clusters that can contribute to the growth of a NSC are very massive systems with relaxation times longer than their dynamical friction timescale this simplification is quite reasonable and does not alter our results in any important way. However, dynamical evaporation due to internal dynamics is also accounted for, in the sense that we do not follow the evolution of clusters which are disrupted (evaporated) on timescales shorter than the relevant dynamical friction timescales.

### 3.2.2. Formation of the MW NSC

Luminosity profiles of galaxies are well approximated by power laws with  $1 < \gamma < 2$  at radii smaller than the effective radius of the stellar spheroid ( $R_{\text{eff}}$ ; Terzić & Graham 2005). Since for MW-like galaxies the only clusters that can reach the GC in one Hubble time are those initially at  $r \lesssim R_{\text{eff}}$  (Milosavljević 2004), and that within these radii the baryonic matter dominates the galactic potential, we represent the galaxy bulge by using a simple power-law density model:  $\rho(r) = \rho_0 (r/r_0)^{-\gamma}$ , with  $\rho_0 = (3-\gamma)M_{\text{sph}}/4\pi r_0^3$ ,  $M_{\text{sph}} = 10^{10} M_\odot$ ,  $r_0 = 700$  pc and  $\gamma = 1$  (e.g., McMillan & Dehnen 2007). The scale length  $r_0$ , is related to the bulge effective radius via  $R_{\text{eff}}/r_0 = (1.8, 1.5, 1)$  for  $\gamma = (1, 1.5, 2)$ . We assume that the clusters have initially the same distribution of stars in the galaxy (e.g., Agarwal & Milosavljević 2011) and we assign their masses using the cluster initial mass function (CIMF),  $dn/dM \propto M^{-2}$  (Bik et al. 2003; de Grijs et al. 2003), and limiting mass values of  $M_{\text{min}} = 10^2 M_\odot$ ;  $M_{\text{max}} = 10^6 - 10^7 M_\odot$ .

The fraction of all star formation that occurs in gravitationally bound stellar clusters is usually referred to as ‘‘cluster formation efficiency’’. The cluster formation

<sup>2</sup> These equations also assume circular orbits. This is consistent with the well known effect of orbital circularization due to dynamical friction (e.g., Casertano et al. 1987; Hashimoto et al. 2003).

<sup>3</sup> This expression assumes that the density follows a Dehnen (1993) profile at large radii, i.e.,  $\rho(r) \sim r^{-4}$  for  $r \gg r_0$ .

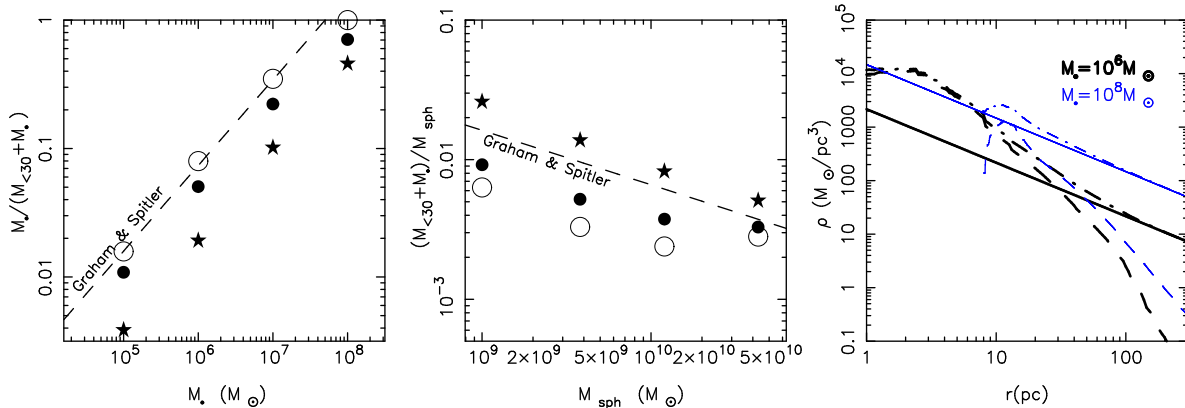


FIG. 2.— Effect of a galactic center MBH on the NSC properties. We assume  $M_{\max} = 10^7 M_{\odot}$  and that the total mass in clusters is initially  $0.05 \times M_{\text{sph}}$  (open circles),  $0.1 \times M_{\text{sph}}$  (filled circles), or  $0.3 \times M_{\text{sph}}$  (star symbols). The properties of the galaxy are changed with  $M_{\bullet}$  according to the observed scaling relations between MBHs and the properties of their host spheroid. In the left panel we plot the ratio  $M_{\bullet}/(M_{\bullet} + M_{<30})$  as a function of  $M_{\bullet}$ , where  $M_{<30}$  is the mass deposited in the inner 30 pc of the galaxy. Dashed line is the observed correlation: equation (1) in Graham & Spitler (2009). This plot measures the relative importance of  $M_{\bullet}$  to the total mass in the nuclear components for different black hole masses. The middle panel gives the importance (in terms of mass) of the nuclear component (MBH + NSC) relative to the host spheroid mass. Dashed line is the observed correlation given by equation (2) in Graham & Spitler (2009). As an example, the right panel displays the density profile of background galaxy (solid lines), NSC (dashed lines) and the sum of them (dot-dashed lines) for an initial total mass in clusters equal to  $0.1 \times M_{\text{sph}}$  and for  $M_{\bullet} = 10^6$  and  $10^8 M_{\odot}$ . Clearly, larger MBHs correspond to NSCs with lower central densities. For  $M_{\bullet} \gtrsim 10^8$ , the NSC densities remain below the density of the galaxy at all radii.

efficiency in the MW is  $\sim 10\%$  (Lada & Lada 2003). Accordingly, in our model we assume that the total mass in clusters is initially  $M_{\text{cl}} = 0.1 \times M_{\text{sph}}$ .

We start by identifying a “dissolution time” for globular clusters due to dynamical evaporation as a function of their initial mass (Baumgardt & Makino 2003; Gieles & Baumgardt 2008; Lamers et al. 2010):

$$t_{\text{dis}} = t_0 \left( \frac{m_{\text{cl}}}{M_{\odot}} \right)^{\beta} \quad (33)$$

with  $\beta = 0.7$ ,  $m_{\text{cl}} = m_t$  if the cluster is truncated,  $t_0 = 0.3 \times |d\Omega/d\ln r|^{-1}$  and  $\Omega$  the angular velocity at the galactocentric radius  $r$ . We then remove clusters with total lifetime,  $t_{\text{dis}}/\beta$ , shorter than the dynamical friction time-scale,  $\tau_{\star}$ . This procedure reduces the initial total mass in globular clusters from  $10^9 M_{\odot}$  to  $\sim 5 \times 10^7 M_{\odot}$  for  $M_{\max} = 10^6 M_{\odot}$ , and to  $\sim 2 \times 10^8 M_{\odot}$  for  $M_{\max} = 10^7 M_{\odot}$ . By comparing equation (32) with equation (33) one can easily show that if  $\gamma \lesssim 3/2$  and  $t_{\text{dis}}/\beta > \tau_{\star}$  initially, this latter condition remains satisfied during inspiral.

We set the core radius of the globular clusters to be  $r_K = 1$  pc, roughly equal to the median value of the core radii listed in the Harris’s compilation (Harris 1996) of Galactic globular clusters. If a cluster reached its tidal disruption radius its core mass is redistributed uniformly at the radius of disruption over a region of extent  $r_{\text{disp}} = 3$  pc. But we note that our results do not strongly depend on the particular value for this parameter, which only affects the NSC density profile at very small radii ( $\lesssim 3$  pc). Within these central regions we expect that other dynamical processes (e.g., two-body relaxation, mass segregation) will modify the NSC density profile with respect to the simple predictions of our Monte-Carlo experiments (we discuss this point in more detail below). When a cluster enters the inner 1 pc, its mass was redistributed using a Plummer sphere model of total mass  $m_t(1\text{pc})$  and core radius  $r_K$ .

In addition, we make the reasonable assumption that

the distribution of field stars is constant when computing the relevant dynamical friction time-scales. Given that the total mass in clusters is only 10% of the bulge mass initially, the density profile of the galaxy at intermediate and large radii ( $\gtrsim 30$  pc; e.g., see Figure 4 of Agarwal & Milosavljević 2011) and consequently the dynamical friction timescales are not significantly affected by such simplification. However, to approximately account for the mass that is progressively accumulated into the nucleus, the orbital decay of clusters was computed in order of increasing migration time; then, for any inspiral, we added the quantity  $3GM_{\text{acc}}(< r)/r^3$  to the terms in square brackets in equation (23), with  $M_{\text{acc}}(< r)$  the accumulated mass within  $r$  due to clusters with shorter orbital decay times.

Finally, we computed the NSC density at any radius by summing up the contribution,  $\Delta\rho(r)$ , of all clusters that within  $10^{10}$  yr reached that radius. After this time the total mass left in stellar clusters is  $\sim 10^7 M_{\odot}$ , almost independent on the initial value of  $M_{\max}$ . The initial mass of the globular cluster system is therefore reduced from 10 % to 0.1 % of the total Bulge mass after one Hubble time due to dynamical dissolution of the less massive systems, and also due to massive clusters that inspiral into center of the galaxy and dissolve locally to form the stellar nucleus. Figure 1 gives the results of such calculations.

In agreement with Agarwal & Milosavljević (2011) we found that the mass of the forming NSC is mostly ( $\gtrsim 90\%$ ) composed of clusters with initial masses  $\gtrsim 0.1 \times M_{\max}$ , suggesting that the low mass clusters scarcely contribute to NSC formation in galaxies. Instead, our results very much depend on the value of  $M_{\max}$ , since only very massive clusters can arrive in the central regions of the galaxy in a reasonable time without being destroyed by the galactic tidal forces in the process.

In galaxy models without a MBH, NSC formation is more efficient, and even for  $M_{\max} = 10^6 M_{\odot}$  a NSC forms in the central few parsecs of the galaxy. If a MBH



is present at the center of the galaxy, star clusters that come closer than  $r_{\text{disr}}$  from the center are disrupted and, as a result, the NSC density is limited inside this radius (left panels in the Figure 1). For a MBH mass of  $4 \times 10^6 M_{\odot}$  and  $M_{\text{max}} = 10^6 M_{\odot}$ , no clusters penetrate radii smaller than  $\sim 7$  pc. From the lower-left panel in Figure 1 we can see that, in this case, the presence of a MBH will strongly inhibit the formation of a NSC. Taking  $M_{\text{max}} = 10^7 M_{\odot}$  (upper-left panel) results in a smaller radius of the NSC core and higher central densities, since the most massive clusters can reach smaller galactocentric radii ( $\sim 2$  pc).

A model that starts with a high mass truncation of  $M_{\text{max}} = 10^7 M_{\odot}$  reproduces the observed mass density profile of stars in the Galactic NSC (red-dotted lines in Figure 1) outside 3 pc. We conclude that a scenario in which a large fraction of the mass of the Milky Way NSC is due to infalling globular clusters is in good agreement with current observational constraints.

The results presented here should be interpreted with caution when comparing the detail of the NSC density profile to observations. Our modeling includes a series of simplifications that can have some impact on the inner structure of the resulting NSC. For example, consideration of the internal dynamics and mass spectrum in the globular clusters could enable mass segregation which can increase  $\sigma_K$  and then allow the cluster stars to reach much smaller radii. A realistic treatment of these effects will require careful  $N$ -body simulations and is beyond the scope of this paper. Nevertheless, we note that the results of our computations that include a central MBH are very similar to those obtained in Antonini et al. (2012) via  $N$ -body simulations. In both cases, the density profile that results after the final inspiral event is characterized by a core of roughly the tidal disruption radius of the most massive clusters,  $\sim 3$  pc, and an envelope with density that falls off as  $\rho \sim r^{-2}$ . These properties are similar to those of the MW NSC, with the exception of the core size, which in the MW is somewhat smaller ( $\sim 0.5$  pc). Merritt (2010) showed that such a core will shrink substantially via gravitational encounters in a time of 10 Gyr as the stellar distribution evolves toward a Bahcall-Wolf cusp (Bahcall & Wolf 1976). In our computations cluster inspiral occurs more or less continuously over the lifetime of the galaxy. The core resulting from the combined effects of cluster inspiral and relaxation would therefore be somewhat smaller than that we found above, and closer to the observed core size (we discuss this point in more details below in §6.1).

### 3.2.3. The role of MBHs

Figure 2 shows the results of additional computations that explore the effect that varying  $M_{\bullet}$  has on the structure of the NSC. In these plots we set  $M_{\text{max}} = 10^7 M_{\odot}$  and we relate the mass of the galaxy to  $M_{\bullet}$  through the relation  $\log[M_{\bullet}/M_{\odot}] \approx 8.4 + 1.9 \log[M_{\text{sph}}/7 \times 10^{10} M_{\odot}]$  (Graham 2012b). The galaxy velocity dispersion,  $\sigma$ , is derived from the  $M_{\bullet} - \sigma$  relation (Ferrarese & Merritt 2000; Gebhardt et al. 2001), while the model scale length,  $r_0$ , is obtained from the effective radius:  $R_{\text{eff}} \approx 1 \text{ kpc} (M_{\text{sph}}/10^{10} M_{\odot})/(\sigma/100 \text{ km s}^{-1})^2$ , where here the normalization reproduces approximately the observed ef-

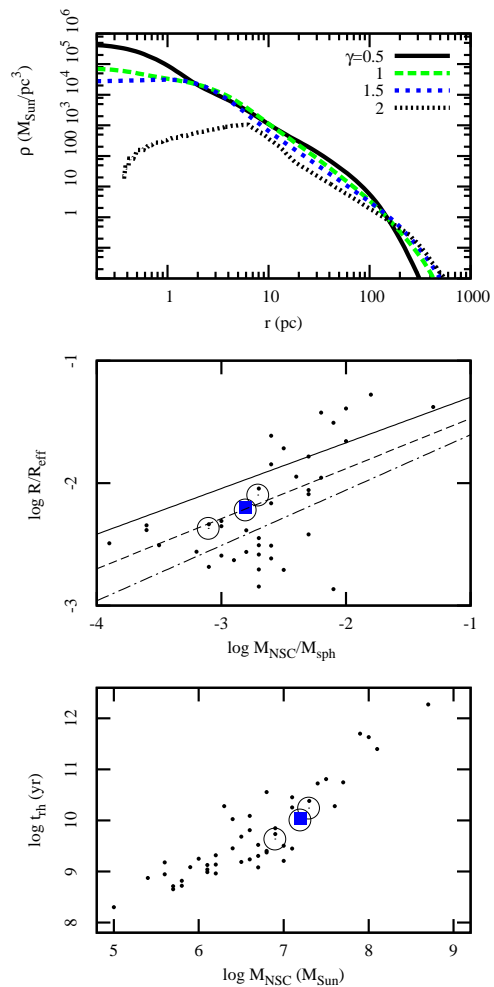


FIG. 3.— Upper panel gives the density profile of NSCs after  $10^{10}$  yr in galaxy models with inner density profile slope  $\gamma = (0.5, 1, 1.5, 2)$ . In these computations we set  $M_{\text{sph}} = 10^{10} M_{\odot}$ ,  $R_{\text{eff}} = 1$  kpc,  $M_{\bullet} = 0$ , and  $M_{\text{cl}} = 0.1 \times M_{\text{sph}}$ . The high mass truncation of the CIMF is  $M_{\text{max}} = 10^7 M_{\odot}$ . The largest NSC central densities are found in models with small values of  $\gamma$ . In the middle and lower panels the properties of the NSC models are compared to those of real NSCs in early type galaxies (dots are data from Côté et al. 2006; Seth et al. 2008). The middle panel plots the nuclei in the size ratio versus mass ratio plane. Open circles correspond to the NSC models of the top panel with  $\gamma = (0.5, 1, 1.5)$ , where the relaxation time and effective radius of the NSC decrease with increasing  $\gamma$ . The blue-filled squares represent the model in the upper right panel of Figure 1. Lines indicate the critical value of  $R/R_{\text{eff}}$  over which nuclei expand for galaxy models described by Einasto indices  $n = 2$  (continue line),  $n = 3$  (dashed line) and  $n = 4$  (dot-dashed line), (for comparison see Figure 1c in Merritt 2009). The lower panel shows the dependence of NSC half-mass relaxation time on its total mass.

fective radii of elliptical galaxies (Forbes et al. 2008; Graham & Worley 2008). In the left panel of Figure 2 we show the increasing dominance of the central MBH over the NSC stars for more massive galaxies. Our results agree reasonably well with studies of galaxies at high mass end with  $M_{\bullet} > 10^8 M_{\odot}$ , and which exclude the presence of stellar nuclei in such systems (e.g., Häring & Rix 2004). The middle panel of Figure 2 dis-



plays how the total central mass in the nuclear component (i.e., MBH + NSC) divided by the stellar mass of the host spheroid varies with this latter quantity. Also in this case our results agree reasonably well with the observed correlation (dashed line in the plot).

In order to reproduce the NSC masses obtained from observations, our model would require a high mass truncation of the CIMF of  $M_{\max} = 10^7 M_{\odot}$  and that  $\lesssim 10\%$  of stars in galaxies originate in stellar clusters. Such a result is in agreement with the conclusion of Leigh et al. (2012) that the globular cluster infall model strongly under-predicts the observed NSC masses when assuming the present day number of globular clusters in galaxies. This assumption might be incorrect however, given that the number of globular clusters in a galaxy drops rapidly with time due to dynamical disruptions (e.g., Vesperini 1997, 1998; Fall & Zhang 2001; Gieles 2009). In addition, the cluster formation efficiency and the cluster disruption rate also vary substantially with cosmic time, peaking at early epochs, in gas-rich disk galaxies (Kruijssen et al. 2012). In fact, up to 30 per cent of all stars in the Universe could have been formed in bound stellar clusters (Kruijssen 2012).

The right panel of Figure 2 gives the density profile of a NSC that forms around a MBH of mass  $M_{\bullet} = 10^6 - 10^8 M_{\odot}$  assuming an initial mass in clusters  $M_{\text{cl}} = 0.1 \times M_{\text{sph}}$ . Smaller black hole masses correspond to smaller tidal disruption radii for the infalling globular clusters. As a consequence, the NSC peak density becomes progressively larger and the NSC core radius smaller as  $M_{\bullet}$  decreases. The mass delivered in the inner region of the galaxy is also a strong function of  $M_{\bullet}$ . For  $M_{\bullet} \gtrsim 10^8 M_{\odot}$ , very little mass ( $\lesssim 10^6 M_{\odot}$ ) can be deposited in the inner  $\sim 30$  pc of the galaxy. In this case the NSC density profile remains below the stellar density of the background galaxy.

To summarize the results presented in this section, if we postulate that NSCs grow slowly through globular cluster migration and merging, then in order to form a NSC similar to that of the MW, our model will require  $M_{\max} \sim 10^7 M_{\odot}$  and that  $\sim 10$  per cent of the Bulge mass originated in stellar clusters. We showed that this fraction reduces to roughly 0.1 % of the total Bulge mass after  $10^{10}$  yr due to dynamical evaporation of the less massive clusters, and also because more massive clusters inspiral toward the galactic center and dissolve due to their interaction with the galactic tidal field.

The presence of a pre-existing MBH at the center of the galaxy can have a strong impact on the inner structure of the forming nucleus. If a MBH of mass  $M_{\bullet} \sim 10^6 M_{\odot}$  sits at the center of the galaxy, massive globular clusters are disrupted at radii of order  $\sim 3$  pc and the NSC density profile will have a core of roughly this radius. MBHs less massive than about  $10^6 M_{\odot}$  do not influence very much the structure of the stellar nucleus during its formation since the tidal disruption radius of massive GCs is in this case of the order (or less than) the core radius of the most massive clusters, and in either models, with or without MBH, the NSC density profile will have a central core of typical size  $r_k$ . In low mass spheroids after a few Gyr such a core will most likely relax to a Bahcall-Wolf cusp or, in the absence of MBH, undergo core-collapse. The central peak density of the resulting

NSC progressively declines as  $M_{\bullet}$  increases. NSCs forming around MBHs with  $M_{\bullet} \gtrsim 10^8 M_{\odot}$  have such low central densities that they would be more difficult to observe as distinct galactic components; this appears to be in agreement with observations which reveal a lack of NSCs in stellar spheroids brighter than about  $10^{10.5} L_{\odot}$ .

#### 4. DEPENDENCE ON $\gamma$

In the above discussion we have considered Dehnen's models with inner density profile slope  $d \log \rho / d \log r = -1$ . In Figure 3 we relax this assumption and explore the formation of NSCs in galaxy models with different values of  $\gamma$ . In these computations we adopt  $M_{\max} = 10^7 M_{\odot}$  and  $M_{\text{cl}} = 0.1 \times M_{\text{sph}}$ . The structural parameters defining the galaxy model are  $M_{\text{sph}} = 10^{10} M_{\odot}$ ,  $R_{\text{eff}} = 1$  kpc, and  $M_{\bullet} = 0$ .

On the basis of equation (26) we would expect the final (after  $10^{10}$  yr) densities in the inner  $\sim 100$  pc of the forming NSC to be lower in galaxy models with steeper density profiles, provided that the dynamical friction timescale of massive stellar clusters remains shorter than the Hubble time. The results illustrated in the upper panel of Figure 3 agree with this basic prediction, suggesting that, independently on  $\gamma$ , the sinking timescale of massive clusters in these models is short enough that they can always reach the center of the galaxy and form a compact nucleus.

The middle and bottom panels in Figure 3 compare the structural properties of our model NSCs to the properties of NSCs in early-type galaxies that were found to be nucleated in Côté et al. (2006). For each of the NSC models an approximation of its effective radius is obtained as the effective radius of the best fitting Sérsic model to the NSC projected density profile within a galactocentric radius of 30 pc. Given  $R$ , the total NSC mass,  $M_{\text{NSC}}$ , is then obtained as the total mass within a radius twice the effective radius. A useful reference time is the relaxation time computed at  $R$ . Setting  $\ln \Lambda = 12$ , and ignoring the possible presence of a MBH, the half-mass relaxation time is (Spitzer 1987):

$$t_{\text{rh}} = 1.75 \times 10^5 \frac{[r_h(\text{pc})]^{3/2} N^{1/2}}{(m/M_{\odot})^{1/2}} \text{yr}, \quad (34)$$

where  $N$  is the total number of stars and  $m$  is the mass of a single star ( $m = M_{\odot}$  in Figure 3). From Figure 3 it is evident that our NSC models have structural properties that are similar to those of real nuclei.

In the absence of a central MBH the dynamical evolution of a nuclear cluster is a competition between core collapse, which causes densities to increase, and heat input from the surrounding galaxy, which causes the cluster to expand and densities to decrease (Kandrup 1990; Quinlan 1996; Merritt 2009). In a double-Plummer-law galaxy model, the maximum size of a NSC of mass  $M_{\text{NSC}}/M_{\text{sph}} = 10^{-3}$  in order to resist expansion is  $R/R_{\text{eff}} \approx 0.02$  (Quinlan 1996). This simple condition, when compared to the middle panel of Figure 3, implies that the core-collapse time of our models are always shorter than the time for the nucleus to absorb energy from the rest of the galaxy. However, when using more realistic Einasto profiles to describe the surrounding galaxy our NSC models appear to be close to the transition region between systems that are in the prompt

core collapse phase and systems for which the evolution is driven by heating from the galaxy. Our models will therefore either expand or contract depending on the “compactness” of the surrounding galaxy.

## 5. ORBITAL DECAY IN THE CORE OF A GIANT ELLIPTICAL GALAXY

Stellar spheroids more luminous than  $\sim 10^{10.5} L_{\odot}$  often host high mass black holes ( $M_{\bullet} \gtrsim 10^9 M_{\odot}$ ) at their center, while they show no evidence for nucleation. Rather, the density profile of such “giant” elliptical galaxies is observed to be flat inside the influence radius of the MBH (Kormendy 1987; Lauer et al. 2002). Two factors have been invoked to explain the observed lack of NSCs in such systems: (i) NSCs and MBHs grow in competition from the same gas reservoir (Escala 2007). If a MBH forms first this can prevent, through its feedback, a NSC from growing if the gas accretion rate is smaller than the Eddington rate (Nayakshin et al. 2009). (ii) Massive black hole binaries forming during the last galaxy-galaxy major merger destroyed their host NSCs by ejecting stars from the inner galactic regions (Bekki & Graham 2010).

Observations seem to point against both scenarios. Picture (i) seems to break down for NSC-dominated galaxies, given the extremely low accretion rates observed in bulgeless galaxies and that at least few of them also contain central MBHs. The model of Bekki & Graham (2010) is disfavored due to the fact that what sets NSC disappearance does not seem to be galaxy morphology. Rather, there is a limit to the MBH/NSC mass ratio that fixes a sharp transition from galaxies with NSC and MBH-dominated galaxies (Neumayer & Walcher 2012).

Of course, it is possible that nuclei are absent in bright galaxies because some mechanism prevents them from forming in the first place, or because they did not have time to reform after they were destroyed by the scouring effect of binary black holes. In what follows, we show that NSCs might in fact be difficult to form in such galaxies, due to long dynamical friction time-scales of star clusters and also the little mass that the clusters can deliver to the center due to the strong MBH tidal field. In order to do so, we repeat a similar analysis to that presented in § 3.2.2 but for a galaxy like M87, a giant elliptical with no evidence for NSC. We stress that the problems discussed here and in § 3.2.2 are substantially different. The influence radius of the MBH in a galaxy like M87 extends much further out (a few hundreds of parsecs from the center) than the tidal disruption radius of a massive globular cluster ( $\sim 10$  pc), while for the MW we found  $r_{\text{disr}} \lesssim r_{\text{infl}}$ . In the former case, the clusters will therefore move in a stellar background whose velocity distribution is directly influenced by the presence of a MBH, which will strongly affect the timescale for cluster inspiral as we now show.

The distribution of field-star velocities has the following form near a MBH:

$$f(v_{\star}) = \frac{\Gamma(\gamma + 1)}{\Gamma(\gamma - \frac{1}{2})} \frac{1}{2^{\gamma} \pi^{3/2} v_c^{2\gamma}} (2v_c^2 - v_{\star}^2)^{\gamma-3/2}, \quad (35)$$

where the normalizing constant corresponds to unit total number. This expression gives the local distribution

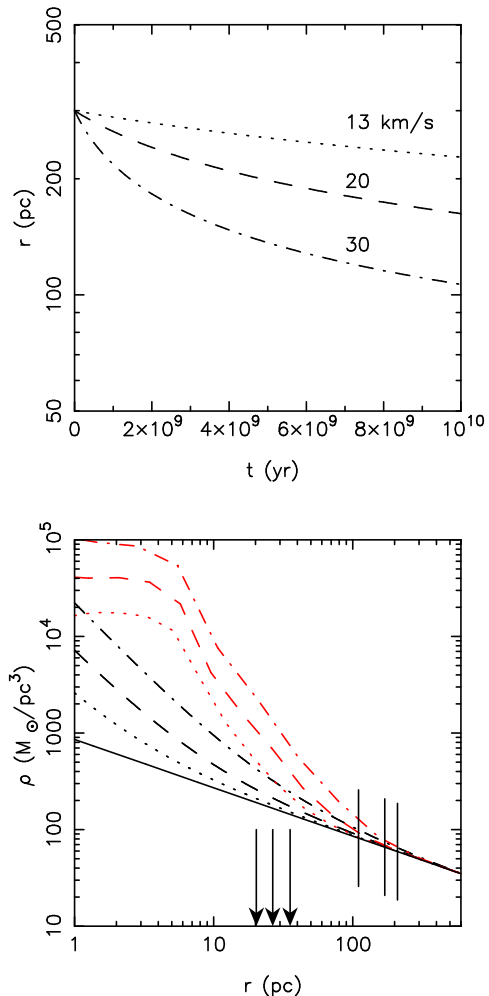


FIG. 4.— Upper panel gives the orbital evolution of clusters with different values of the central velocity dispersion in the core of a M87-like galaxy. The dynamical friction timescale for clusters in such models is very long due to the lack of stars that move slower than the local circular velocity inside  $r_{\text{infl}}$ . Even after  $10^{10}$  yr the cluster orbital radii have hardly changed from their initial values. The lower panel gives the density profile of the galaxy, assuming that the clusters did have enough time to migrate to the center: dotted, dashed and dot-dashed curves show the results of the accumulation of 500 clusters with  $\sigma_K = 13$ ; 20 and 30  $\text{km s}^{-1}$  respectively. Red lines correspond to computations without a MBH at the center of the galaxy. The galaxy background model is shown as a solid black line. Vertical marks correspond to the orbital radius of the cluster in the model with an MBH after  $10^{10}$  yr and starting from  $r_{\text{infl}} = 300$  pc. Arrows give the tidal disruption radii of the clusters due to the MBH. At radii smaller than these our computations including a MBH are no longer valid.

of velocities at a radius where the circular velocity is  $v_c = (GM_{\bullet}/r)^{1/2}$ , assuming that the density of field stars follows  $\rho(r) = \tilde{\rho}(r/\tilde{r})^{-\gamma}$ . The phase space density is zero for  $v_{\star} \geq v_{\text{esc}} = 2^{1/2}v_c$ .

As  $\gamma \rightarrow 1/2$  the velocity distribution (35) becomes progressively narrower, and for  $\gamma = 1/2$  all stars have zero energy; in other words, the number of stars with  $v_{\star} < v_c$  goes to zero as  $\gamma$  approaches  $1/2$ . In the case of a test particle moving in a circular orbit the standard Chandrasekhar’s formula will therefore predict zero frictional force. It turns out that in this situation the frictional force must be computed using a more general formulation that also includes the contribution from stars mov-

ing faster than the test particle:

$$\begin{aligned} \mathbf{f}_{\text{df}} \approx \mathbf{f}_{\text{df}}^{(v_* < v)} + \mathbf{f}_{\text{df}}^{(v_* > v)} = & \\ -4\pi G^2 m_{\text{cl}} \rho(r) \frac{\mathbf{v}}{v^3} \times \left( \ln \Lambda \int_0^v dv_* 4\pi f(v_*) v_*^2 \right. & \\ \left. + \int_v^{\sqrt{-2\phi(r)}} dv_* 4\pi f(v_*) v_*^2 \left[ \ln \left( \frac{v_* + v}{v_* - v} \right) - 2 \frac{v}{v_*} \right] \right), & \end{aligned} \quad (36)$$

where  $\mathbf{v}$  is the velocity of the infalling cluster. The second term in parentheses represents the frictional force produced by stars moving faster than the massive particle.  $N$ -body experiments verify the accuracy of this formula (Antonini & Merritt 2012).

The fraction of stars that move slower than the local circular velocity can be computed as

$$\begin{aligned} I_{v_* < v_c} &= \int_0^{v_c} dv_* 4\pi f(v_*) v_*^2 \\ &= \frac{2}{\sqrt{\pi}} \frac{\Gamma(\gamma + 1)}{\Gamma(\gamma - 1/2)} \int_{1/2}^1 dx x^{\gamma-3/2} \sqrt{1-x}, \end{aligned} \quad (37)$$

This function varies smoothly from 0 when  $\gamma = 0.5$  to 0.5 when  $\gamma = 2$ . For the fast moving stars an (ad-hoc) approximation is

$$\begin{aligned} I_{v_* > v_c} &= \int_{v_c}^{\sqrt{-2\phi(r)}} dv_* 4\pi f(v_*) v_*^2 \left[ \ln \left( \frac{v_* + v_c}{v_* - v_c} \right) - 2 \frac{v_c}{v_*} \right] \\ &\simeq 0.1721 + 0.5280\gamma - 0.1812\gamma^2 - 529.2 \exp(-14.46\gamma). \end{aligned}$$

For  $\gamma > 1$ ,  $I_{v_* > v_c} \sim 0.53$ , and when  $\gamma \sim 2$  the contribution from the slow stars is of order  $\sim \ln \Lambda$  larger than the frictional force due to the fast moving stars.

Given these expressions, and setting  $L = \sqrt{GM_\bullet r}$  in equation (3) we have

$$\frac{dr}{dt} = -\frac{8\pi\sqrt{G}\tilde{\rho}\tilde{r}^\gamma}{M_\bullet^{3/2}} \times [\ln \Lambda I_{v_* < v_c} + I_{v_* > v_c}] m_{\text{cl}} r^{5/2-\gamma}. \quad (38)$$

This expression can be then used to compute orbits for both point-like and extended objects (e.g., a stellar cluster that experiences mass loss during inspiral) that move in a stellar cusp near a MBH. We identified our model with the center of a galaxy like M87. We adopted  $M_\bullet = 3 \times 10^9 M_\odot$  (Macchetto et al. 1997; Gehardt et al. 2011), a core velocity dispersion  $\sigma_h = 278 \text{ km s}^{-1}$  (Young et al. 1978; Lauer et al. 1992) and we used the relation  $\sigma_h^2 = 4\pi G \rho_h (r_h/3)^2$  with  $r_h = 600 \text{ pc}$  to obtain the core density:  $\rho_h = 35 M_\odot \text{ pc}^{-3}$ . Taking  $\gamma = 0.5$ , the density at  $\tilde{r} = r_{\text{infl}} = 300 \text{ pc}$  is  $\tilde{\rho} = 50 M_\odot \text{ pc}^{-3}$ .

For a test particle of mass  $m_{\text{cl}}$ , integrating equation (38) yields

$$\begin{aligned} r(t) &= \left[ r_{\text{in}}^{\gamma-3/2} - \frac{8\pi\sqrt{G}\tilde{\rho}\tilde{r}^\gamma(\gamma-3/2)}{M_\bullet^{3/2}} \right. \\ &\quad \left. \times [\ln \Lambda I_{v_* < v_c} + I_{v_* > v_c}] m_{\text{cl}} \times t \right]^{\frac{1}{\gamma-3/2}}, \end{aligned} \quad (39)$$

for  $\gamma \neq 3/2$ , and

$$r(t) = r_{\text{in}} \exp \left( -\frac{8\pi\sqrt{G}\tilde{\rho}\tilde{r}^\gamma}{M_\bullet^{3/2}} [\ln \Lambda I_{v_* < v_c} + I_{v_* > v_c}] m_{\text{cl}} \times t \right) \quad (40)$$

for  $\gamma = 3/2$ .

Equation (39) corresponds to a characteristic decay time for angular momentum loss (for  $\gamma > 3/2$ ):

$$\begin{aligned} \tau_\bullet &= 4 \times 10^8 \text{ yr} \frac{[\ln \Lambda I_{v_* < v_c} + I_{v_* > v_c}]^{-1}}{\gamma - 3/2} \\ &\quad \times M_{\bullet,9.5}^{3/2} \tilde{\rho}_{50}^{-1} \tilde{r}_{300}^{-3/2} m_{\text{cl},6}^{-1} \left( \frac{r_{\text{in}}}{\tilde{r}} \right)^{\gamma-3/2} \end{aligned} \quad (41)$$

where  $M_{\bullet,9.5} = M_\bullet/3 \times 10^9 M_\odot$ ,  $\tilde{\rho}_{50} = \tilde{\rho}/50 M_\odot \text{ pc}^{-3}$ , and  $\tilde{r}_{300} = \tilde{r}/300 \text{ pc}$ . We note that, for  $\gamma < 3/2$ ,  $\tau_\bullet$  becomes negative and, formally, equation (38) gives an infinite decay time to the center. In this latter case the dynamical friction timescale can be re-defined as the time required to reach a radius which is some fraction,  $\zeta$ , of its initial value:  $\tau_\bullet \times (1 - \zeta^{\gamma-3/2})$ , with  $\tau_\bullet$  from equation (41).

In the case of extended objects, we assume that the central properties of the globular cluster (i.e.  $\sigma_K$  and  $r_K$ ) remain unchanged during inspiral. The cluster's limiting radius is given by equation (23), which permits expressing the satellite mass as a function of radius. Setting  $m_{\text{cl}} = m_t$  in equation (38) and assuming that the galactic potential is dominated by the MBH, we obtain

$$\begin{aligned} r(t) &= \left[ r_{\text{in}}^{\gamma-3} - \frac{2^{3/2}\pi\tilde{\rho}\tilde{r}^\gamma(\gamma-3)}{\sqrt{3}GM_\bullet^2} \right. \\ &\quad \left. \times [\ln \Lambda I_{v_* < v_c} + I_{v_* > v_c}] \sigma_K^3 \times t \right]^{\frac{1}{\gamma-3}}, \end{aligned} \quad (42)$$

and

$$\begin{aligned} \tau_\bullet &= 5 \times 10^9 \text{ yr} \frac{[\ln \Lambda I_{v_* < v_c} + I_{v_* > v_c}]^{-1}}{3-\gamma} (\zeta^{\gamma-3} - 1) \\ &\quad \times M_{\bullet,9.5}^2 \tilde{\rho}_{50}^{-1} \tilde{r}_{300}^{-3} \sigma_{K,10}^{-3} \left( \frac{r_{\text{in}}}{\tilde{r}} \right)^{\gamma-3}. \end{aligned} \quad (43)$$

We used equations (39) and (42) to trace the orbital evolution of massive stellar clusters in the core of our galaxy model. We take a limiting value for the mass of  $m_K = 4 \times 10^6 M_\odot$ , corresponding to the non-truncated model, when the cluster is far from the center. The simulated orbits (upper panel of Figure 4) demonstrate that the dynamical friction time-scale in the core of bright elliptical galaxies is extremely long. Also very massive clusters ( $\sigma_K \gtrsim 30 \text{ km s}^{-1}$ ) starting well within the galaxy core ( $r_{\text{in}} \sim 300 \text{ pc}$ ), do not reach the center after one Hubble time.

In the lower panel of Figure 4, we use equations (23) and (26) to compute the density profile of a NSC resulting from the accumulation of 500 equally massive globular clusters in the center of our M87 galaxy model. At radii smaller than  $r_{\text{disr}}$  (marked by black arrows in the plot) the clusters are fully disrupted by the interaction with the MBH and our integrations are no longer valid.  $N$ -body simulations show that the density profile of stars will be very flat or even declining toward the MBH inside

$r_{\text{disr}}$ , as the stars accumulate near the radius of disruption (Kim & Morris 2003; Fujii et al. 2009, 2010).

In order to highlight the role of the central MBH in determining the structure of the growing nucleus Figure (4) also shows the density profile of the nucleus when the mass of the MBH is set to zero. In this case, most of the cluster mass is delivered in the inner  $\sim 100$  pc and consequently the NSC is much more centrally concentrated. After 500 inspiral events, the NSC appears to be distinct from the galaxy background density profile. Apparently, NSCs assembled around MBHs have a spatially more diffuse configuration and lower densities than those forming in galaxies with no MBH. We conclude that the formation of NSCs in giant ellipticals might be inhibited by the presence of their central MBH for two basic reasons: (i) the long dynamical friction timescale of massive objects in the galaxy core; (ii) clusters are disrupted by the strong tidal field of the MBH producing a merger remnant with density profile that rises only modestly above that of the background galaxy.

We note in passing that the latter argument may also apply to the case in which a giant elliptical galaxy accretes a smaller galaxy containing a dense central nucleus. The large cores observed in the central light profile of bright ellipticals are usually interpreted in terms of the scouring effect of MBH binaries forming during major merger events (Milosavljević & Merritt 2001). It is less clear however how such cores can be preserved up to the present epoch despite the large number of minor mergers that are predicted to occur by standard cosmological models. For instance, an M87 like galaxy is expected to have accreted few galaxies of the size of the MW in the last  $\sim 5$  Gyr (Fakhouri et al. 2010). A plausible explanation for the lack of central dense stellar concentrations in the brightest galaxies was provided by Merritt & Cruz (2001). These authors performed high resolution  $N$ -body simulations of the accretion of high-density dwarf galaxies by low-density giant galaxies. They found that the cusp of the secondary galaxy is disrupted during the merger by the giant galaxy MBH tidal field, producing a remnant with a central density that is only slightly higher than that of the giant galaxy initially; removing the black hole from the giant galaxy allowed the smaller galaxy to remain essentially intact and led to the formation of a high central density cusp, contrary to what is observed.

## 6. DISCUSSION

### 6.1. Long term evolution of NSCs around MBHs

In the previous sections we showed that NSCs resulting from the accumulation of globular clusters around MBHs have lower central densities and larger cores than those forming in galaxies without MBHs. Such a result is consistent with the results obtained using more sophisticated  $N$ -body simulations (Antonini et al. 2012).

Our analysis however did not account for the effects of internal dynamics occurring in the NSC during and after its formation. In a preexisting NSC, the presence of a MBH would inhibit core collapse, causing instead the formation of a Bahcall & Wolf (1976) cusp on the two-body relaxation timescale, followed by a slow expansion as stars are tidally disrupted (Merritt 2009). Whether or not a Bahcall-Wolf cusp will form depends on the initial

core size of the nucleus and on its relaxation time.

For nuclei similar to the MW NSC, relaxation times are too long to assume that they have reached such a collisionally relaxed state, but they are still sufficiently short that gravitational encounters would substantially affect their structure over the age of the galaxy. Two body gravitational interactions will cause the central density of the nucleus to increase and the core to shrink as the stellar distribution evolves toward the Bahcall-Wolf form (e.g., Preto et al. 2004). The time evolution of the core radius can be approximately described by the expression (Antonini et al. 2012)

$$r_{\text{core}}(t) = 1.57 \text{ pc} \exp[t/0.25t_{\text{relax}}] , \quad (44)$$

where  $t_{\text{relax}}$  is the relaxation time computed at the radius of influence of the MBH. For the MW,  $t_{\text{relax}} \sim 20$  Gyr and  $M_{\bullet} \approx 4 \times 10^6 M_{\odot}$ . A black hole of this mass corresponds to a core of  $\sim 3$  pc (Figure 1). From equation (44), we see that gravitational encounters occurring during and after the formation of the NSC will reduce the core size to  $\sim 1$  pc after  $10^{10}$  yr. Such a value is more consistent with the size of the core observed in the distribution of late-type (old) stars in the inner parsec of the MW (Buchholz et al. 2009; Do et al. 2009; Bartko et al. 2010; Yusef-Zadeh et al. 2011; Nadeen et al. 2012). Whether NSCs in other “power-law” galaxies will turn out to have stellar cores similar to that of the MW remains to be seen.

### 6.2. The distribution of stellar remnants near MBHs

NSCs containing MBHs are expected to be the main birthplace of gravitational wave (GW) sources for space-based interferometers (Hughes 2003). These include the capture of stellar-mass black holes (BHs) by MBHs, also called “extreme mass-ratio inspirals” (EMRIs; Merritt et al. 2011; Amaro-Seoane et al. 2012). Understanding systems like the MW NSC and their origin is therefore crucial for making predictions about the event rates for low frequency gravitational wave detectors.

Most of the EMRI rate calculations reported in the literature are derived under the assumption that the galactic nucleus had enough time to reach a state of mass segregation, which implies a high density of BHs near the center (e.g. Freitag et al. 2006; Hopman & Alexander 2006; Alexander & Hopman 2009). This appears to be in conflict with observations which suggest an unrelaxed state for the distribution of stars at the GC. Merritt (2010) and Antonini & Merritt (2012) demonstrated that in the absence of an initial cusp in the stars, even after 5 – 10 Gyr the density of BHs could remain substantially below the densities inferred from steady-state models.

All these previous studies, however, assumed that the stellar BHs had the same phase-space distribution initially as the stars. This is most likely to be a poor assumption if a substantial fraction of the NSC mass comes from orbitally decayed globular clusters. In the merger model the resulting distribution of stellar remnants will reflect their distribution in their parent clusters just before they reach the center of the galaxy.

In a dense stellar cluster, BHs formed by the supernova explosions of the most massive stars tend to segregate into the cluster core and form a sub-cluster of BHs

which dynamically decouples from the rest of the cluster (Spitzer 1987). When the central density of BHs becomes large enough, BH-BH binary formation becomes efficient. Subsequent dynamical interactions involving binary BHs and higher multiplicity systems will tend to eject the BHs from the cluster until only a few of them are left (e.g., Downing et al. 2010, 2011; Banerjee et al. 2010).

We may consider two possibilities <sup>4</sup>: (i) the dynamical friction timescale of star clusters is short compared to the encounter driven evaporation timescale of their BH sub-cluster. In this case, the mass-segregated BH sub-clusters, due to their high central densities, can reach galactocentric radii as small as  $\sim 0.1$  pc (Antonini 2012). The preferential removal of stars from the outer parts of the clusters by the strong galactic tidal field might lead to the formation of a NSC with a central over-abundance of BHs when compared to predictions from standard mass functions (Banerjee & Kroupa 2011). (ii) The orbital decay timescale is shorter than the evaporation timescale of the cluster BH sub-system. Most of the BHs will be dynamically ejected in this case before the cluster reaches the center of the galaxy. As a consequence of this, very few BHs are delivered to the vicinity of the MBH.

All of the above mentioned topics require a dedicated study which we defer to a future paper.

### 6.3. Dissipative NSC formation

Our work shows that a purely dissipationless merger scenario can explain, without obvious difficulties, the basic physical properties of NSCs. It is important to note that we adopted a rather idealized model of an isolated galactic spheroid (with/without MBH). This idealized model enabled us to neglect some gradients of the role of galaxy merging in NSC formation which can only be addressed by means of comprehensive cosmological hydrodynamical simulations. Simulations demonstrate that tidal torques in major mergers of gas-rich galaxies can induce rapid inflow of gas into the center of a galaxy followed by intense nuclear starbursts which results in a central light “excess” in the surface brightness profile of the galactic spheroid (e.g., Hopkins et al. 2008, 2009). Unfortunately, the spatial resolution ( $\gtrsim 50$  pc) of current cosmological simulations is not high enough to address the role of galaxy mergers in the context of NSCs, at least for low and low-intermediate mass galaxies. In addition, it is not clear whether this picture would apply to elliptical, early-type galaxies which lack the large gas reservoirs of spirals, and thus should not experience frequent central starbursts.

On the other hand, the fact that the nuclei formation histories were in part governed by local and dissipative factors is supported by a wide range of observational phenomena. As an example, the gas distribution and the kinematics of the gas in the nearby spiral NGC6946 suggest the presence of a central, small-scale, S-shaped stellar bar which appears to funnel gas towards the galaxy nucleus (within the inner  $\sim 10$  pc) where about  $10^7 M_{\odot}$  of molecular gas have been accumulated. Star forming events triggered by the rapid inflow of gas in the center

of the galaxy may then contribute to the growth of its NSC (Schinnerer et al. 2006). Support to a dissipative origin is added by the fact that NSCs in general tend to have a wide range of stellar ages, including young stellar populations (Rossa et al. 2006; Seth et al. 2006). Our GC contains for instance a large population of young massive stars that most likely formed locally following the infall and fragmentation of a dense gaseous clump in the vicinity of Sgr A\* (Paumard et al. 2006). Such bursts may occur continuously over the age of the Galaxy and thus produce a significant fraction of its NSC mass. Stellar population synthesis studies also show that the GC appears to have undergone continuous and recurrent star formation over the last 10 Gyr, but it is not possible to fit the observations with ancient burst models, such as would be appropriate for an old population of stars that originated in globular clusters (Figer et al. 2004).

Previous work incorrectly used the latter arguments to argue against a dissipationless origin for NSCs (e.g., Milosavljević 2004; Nayakshin et al. 2009). It is important to stress that although observations probe recent and episodic star formation they do not exclude that the bulk of the GC stellar population is in old stars. In fact, the GC luminosity function appears to be consistent with a star formation history in which a large fraction (about 1/2) of the mass consists of old ( $\sim 10$  Gyr) stars and the remainder is due to continuous star formation (Antonini et al. 2012). Accordingly, Pfuhl et al. (2011) found that about 80 per cent of the stellar mass in the inner parsec of the Galaxy is in old stars that formed more than 5 Gyr ago. We add that, although globular clusters in our Galaxy are exclusively old stellar systems (e.g., Rosenberg et al. 1999), this might not be always the case in other galaxies. It is therefore not clear what fraction of the mass in NSCs is contributed by local gaseous fragmentation. More investigation needs to be done in order to explore the implications of in-situ star formation as the origin of galactic nuclei.

### 6.4. NSCs morphology and kinematics

The morphology and kinematics of NSCs are of great importance for understanding their origin (e.g., De Lorenzi 2012).

Aspherical NSCs are commonly observed in external galaxies. Seth et al. (2006) found that the three edge-on late-type galaxies IC 5052, NGC 4206 and NGC 4244 have nuclei that are strongly elongated along the plane of their host galaxies disks. Such clusters show evidence for multiple morphological components, with a disk-like young stellar population superimposed on an older more spherical component. The radial velocity map of the nucleus in NGC 4244, the nearest of these three galaxies ( $D = 4.1$  Mpc), shows evidence for strong rotation,  $30 \text{ km s}^{-1}$  at 10 pc from the center, compared to a central velocity dispersion of  $\sim 28 \text{ km s}^{-1}$  (Seth et al. 2008). There is also evidence for flattening and rotation in the M33 nucleus (Lauer et al. 1998; Matthews et al. 1999). The M33 NSC is elongated along the major-axis of the galaxy and rotates at  $\sim 8 \text{ km s}^{-1}$ , while the central velocity dispersion is  $\sim 27 \text{ km s}^{-1}$  (Gebhardt et al. 2001). The MW NSC also appears to be rotating parallel to the overall Galactic rotation (Trippe et al. 2008; Schödel et al. 2009). Unfortunately, as a consequence

<sup>4</sup> We make here the reasonable assumption that the timescale for a clusters to reach the center of the galaxy is long compared to the mass-segregation timescale of their BH population.

of the strong interstellar extinction along the GC line of sight, our knowledge of the Galactic NSC morphology and size remains very limited.

Is the observed rotation of NSCs consistent with the predictions of a dissipationless model for NSC formation? Of course if a large fraction of the NSC mass was formed via accretion of clusters isotropically distributed throughout the galaxy, no net rotation would be expected, since there will not be any preferred direction for inspiral. If the primary formation process is instead gas accretion from the galactic disk, this would naturally explain both the flattening and the fact that NSCs rotate parallel to their host galaxy rotation.

Although young and rotating components of NSCs might be difficult to reconcile with a globular cluster origin (due to the long time scale for inspiral compared to the ages of the stars), we believe that the evidence for NSC rotation alone, at least in late-type galaxies, is not a strong argument against a dissipationless origin. For instance, clusters falling into the GC could have originated in the inner part of the Galactic disk and they will therefore share in its rotation (Hartmann et al. 2011). Another possibility is that globular clusters crossing the Galactic disk experience a greater frictional force from the increased local stellar/gas density (Bekki 2010) and hence they can be dragged down into the disk plane and transported into the central region of the galaxy where they then accumulate to form a dense nucleus. In either case, the forming NSC will appear to rotate in the same sense of the Galaxy. These hypotheses lead to basic predictions that might be testable with future observations; specifically: (i) NSCs in early-type galaxies, which do not have extended massive disk-like structures, might have slower rotation with respect to NSCs of spiral galaxies. (ii) There should be some mild depletion of stellar clusters in the Galactic disk as compared to off the disk plane <sup>5</sup>.

In conclusion, comparing kinematic data with simulations for distinguishing between gas and cluster accretion may be difficult, since the detailed structure of simulated NSCs varies in an important way with the orbital initial configuration of the infalling clusters. Future observational work should be able to provide more reliable models for the spatial distribution of globular clusters near the center of galaxies, where timescales for infall are reasonably short.

### 6.5. The lack of NSCs in faint galaxies

Galaxies fainter than  $M_B \sim -12$  do not contain prominent stellar nuclei (van den Bergh 1986). The lack of NSCs in dwarf spheroidals was explained in the context of the merger formation scenario in Goerdt et al. (2006). These authors used high resolution  $N$ -body simulations to study the orbital decay of globular clusters in dark matter halos with a core-density structure in the central regions, similar to what inferred by observations (Pryor & Kormendy 1990). In these models the standard Chandrasekhar's dynamical friction formula breaks down (Tremaine & Weinberg 1984; Weinberg 1986) and one finds that a massive object stalls at roughly the dark matter core radius (e.g., Read et al. 2006; Inoue 2009); the number of globular clusters pre-

dicted to inspiral would be then  $\lesssim 1$ . This suggests that the lack of NSCs in the fainter spheroidals could be simply a consequence of the arbitrarily long sinking timescales of stellar clusters in these systems.

Alternatively, the lack of nuclei in faint galaxies could be related to the small total number, or even absence, of globular clusters in these galaxies. In the Local Group, globular clusters seem in fact to disappear in stellar spheroids fainter than  $M_B \sim -12.5$  (e.g., Peng 2008), which would make the formation of NSCs through globular cluster merging impossible in these systems (see also Turner et al. 2012).

## 7. CONCLUSIONS

In this paper we considered a dissipationless formation model for NSCs where globular clusters orbital decay and merge at the center of a galaxy to form a compact nucleus. Our main results are summarized below.

- 1 The observed scaling relation between NSC masses and the velocity dispersion of their host spheroids, the  $M_{\text{NSC}} - \sigma$  relation, is difficult to reconcile with a purely dissipative formation model for the nuclei. These models predict that  $M_{\text{NSC}}$  is a steeply rising function of  $\sigma$ . The observed  $M_{\text{NSC}} - \sigma$  relation is instead in agreement with the predictions of a dissipationless formation model. Dissipationless formation modes produce relations that are substantially shallower than the corresponding MBH scaling relations and are therefore more consistent with observations.
- 2 The globular cluster merger model, in the absence of a central MBH, naturally reproduces the observed relation between the size of galactic nuclei and their total luminosity,  $R \propto \sqrt{L_{\text{NSC}}}$ . When a MBH is present, the dependence of the NSC radius on its mass is substantially weaker than the observed relation because the size of the NSC is mainly determined by the fixed tidal field of the MBH.
- 3 We derived explicit expressions for the orbits of globular clusters owing to dynamical friction and subject to mass-loss due to their tidal interaction with the galaxy (equation 31) or with a central MBH (equation 42). These expressions were used to (i) address the possibility that NSCs in galaxies similar to the MW could have been assembled via cluster migration and mergers; and (ii) to follow the orbital evolution of globular clusters in the core of bright elliptical galaxies.
- 4 NSCs that form through the mergers of globular clusters have a density profile characterized by a parsec-scale core and an envelope that falls off as  $\rho \sim r^{-2}$ . These properties are similar to those of the MW NSC. A NSC with mass comparable to that of the MW NSC is obtained by assuming an initial total mass in stellar clusters which is consistent with the cluster formation efficiency inferred from observational studies of embedded clusters in Galactic molecular clouds (Figure 1).

<sup>5</sup> I am thankful to A. Madigan for pointing this out.

- 5 A pre-existing MBH at the center of the stellar spheroid has a strong impact on the structure of the growing stellar nucleus (Figure 2). Tidal stresses from a MBH disrupt the clusters when they pass within their tidal disruption radius,  $r_{\text{disr}}$ , limiting the density within that radius. Hence, the density profile of the resulting NSC will also have core size of  $\sim r_{\text{disr}}$ . Removing the MBH from the galaxy allows the stellar clusters to keep their inner structure almost unchanged leading to the formation of a NSC with higher peak densities. We find that separating the contribution of the nucleus from that of the galaxy could more difficult in stellar spheroids with more massive MBHs.
- 6 For globular clusters orbiting in the core of a massive elliptical galaxy like M87, the timescale to reach the center is much longer than one Hubble time (Figure 4). The essential reason for this is that the phase-space density of a shallow density cusp of stars around a MBH falls to zero at low energies: inside the galaxy core there are no stars

at any radius that move slower than the local circular velocity. The standard Chandrasekhar's formula predicts little or even no frictional force in this case. In addition, when a MBH is included, the tidal field near  $r_{\text{infl}}$  becomes much stronger, resulting in faster mass loss and fewer stars deposited to the center. Based on these facts, we conclude the presence of central MBHs might inhibit the formation of compact nuclei in the brightest galaxies, in agreement with what is observed.

I am grateful to D. Merritt for numerous discussions about the ideas presented in this paper and for his detailed comments to an earlier version of this manuscript. I thank R. Capuzzo-Dolcetta for encouraging me to study this problem, D. Kruijssen and A. Madigan for useful discussions and M. Alvarez and A. Graham for their comments to an earlier version of this paper. This material is based upon work supported in part by the National Science Foundation Grant No. 1066293 and the hospitality of the Aspen Center for Physics.

## REFERENCES

- Agarwal, M. & Milosavljević 2011, ApJ, 729, 35  
 Alexander, T., & Hopman, C. 2009, ApJ, 697, 1861  
 Amaro-Seoane, P. et al. 2012, CQGra, 2914016  
 Antonini, F. & Merritt, D. 2012, ApJ, 745, 83  
 Antonini, F., Capuzzo-Dolcetta, R., Mastrobuono-Battisti, A. & Merritt, D. 2012, ApJ, 750, 111  
 Antonini, F. 2012, in preparation  
 Balcells, M., Graham, A. W., & Peletier, R. F. 2007, ApJ, 665, 1084  
 Baumgardt, H., & Makino, J. 2003, MNRAS, 340, 227  
 Bahcall, J. N., & Wolf, R. A. 1976, ApJ, 209, 214  
 Bartko et al. 2010, ApJ, 708, 834  
 Bekki, K. & Graham, A. 2010, ApJ, 714, L313  
 Bekki, K. 2010, MNRAS, 401, 2753  
 Banerjee, S., & Kroupa, P. 2011, ApJ, 741, L12  
 Banerjee, S., Baumgardt, H., Kroupa, P. 2010, MNRAS, 402, 371  
 Böker, T., Laine, S., van der Marel, R. P., Sarzi, M., Rix, H., Ho, L. C., & Shields, J. C. 2002, AJ, 123, 1389  
 Böker, T., Sarzi, M., McLaughlin, D. E., van der Marel, R. P., Rix, H., Ho, L. C., & Shields, J. C. 2004, AJ, 127, 105  
 Böker, T. 2010, ihea.book, 99  
 Bekki, K., Couch, W. J., Drinkwater, M. J., & Shioya, Y. 2004 ApJ, 610, L13  
 Bekki, K. 2007, PASA, 24, 77B  
 Bik, A., Lamers, H. J. G. L. M., Bastian, N., Panagia, N., & Romaniello, M. 2003, A&A, 397, 473  
 Buchholz, R. M., Schödel, R., & Eckart, A. 2009, A&A, 499, 483  
 Carollo, C. M., Stiavelli, M., de Zeeuw, P. T., & Mack, J. 1997. AJ, 114, 2366  
 Carollo, C. M., Stiavelli, & Mack, J. 1998, AJ, 116, 68  
 Capuzzo-Dolcetta, R., 1993, ApJ, 415, 616  
 Capuzzo-Dolcetta, R., Miocchi, P., 2008, MNRAS, 388, L69  
 Casertano, S., Phinney, E. S., & Villumsen, J. V., 1987, IAU Symp. 127, Structure and Dynamics of Elliptical Galaxies, ed. T. de Zeeuw (Dordrecht: Reidel), 475  
 Chandrasekhar, S. 1943, ApJ, 97, 255  
 Côté et al. 2006 ApJS, 165, 57  
 de Grijs, R., Anders, P., Bastian, N., Lynds, R., Lamers, H. J. G. L. M., & O'Neil, E. J. 2003, MNRAS, 343, 1285  
 Dehnen, W. 1993, MNRAS, 265, 250  
 De Lorenzi, F., Hartmann, M., Debattista, V. P., Seth, A. C., & Gerhard, O. 2012, arXiv:1208.2161  
 Do, T., Ghez, A. M., Morris, M. R., Lu, J. R., Matthews, K., Yelda, S., & Larkin, J. 2009, ApJ, 703, 1323  
 Downing, J. M. B., Benacquista, M. J., Giersz, M., & Spurzem, R. 2010, MNRAS, 407, 1946  
 Downing, J. M. B., Benacquista, M. J., Giersz, M., & Spurzem, R. 2011, MNRAS, 416, 133  
 Emsellem, E. & van de Ven, G. 2008, ApJ, 674, 653  
 Escala, A. 2007, ApJ, 671, 1264  
 Fakhouri, O., Ma, C., & Boylan-Kolchin, M. 2010, MNRAS, 406, 2267  
 Ferrarese, L. et al. 2006, ApJ, 644, L21  
 Ferrarese, L., & Ford, H. 2005, SSRv, 116, 523  
 Ferrarese, L., & Merritt, D. 2000, ApJ, 539, L9  
 Figer, D. F., Rich, R. M., Kim, S. S., Morris, M., & Serabyn, E. 2004, ApJ, 601, 319  
 Freitag M., Gürkan M. A., Rasio F. A. 2006, MNRAS, 368, 141  
 Fall, S. M., & Zhang, Q. 2001, ApJ, 561, 751  
 Forbes, D. A., Lasky, P., Graham, A. W., & Spitler, L. 2008, MNRAS, 389, 1924  
 Fujii, M., Iwasawa, M., Funato, Y., & Makino, J. 2009, ApJ, 695, 1421  
 Fujii, M., Iwasawa, M., Funato, Y., & Makino, J. 2010, ApJ, 716, L80  
 Gebhardt, K., et al. 2001, ApJ, 539, L13  
 Gebhardt, K., et al. 2001, AJ, 122, 2469  
 Gebhardt, K., et al. 2011, ApJ, 2, 119  
 Genzel, R. et al. 2003, ApJ, 594, 812  
 Goerdt, T., Moore, B., Read, J. I., Stadel, J., & Zemp, M. 2006, MNRAS, 368, 1073  
 Ghez, A. M. et al., 2008, ApJ, 689, 1044  
 Gieles, M. 2009, MNRAS, 394, 2113  
 Gieles, M., & Baumgardt, H. 2008, MNRAS, 389, L28  
 Gillessen, S., Eisenhauer, F., Trippe, S., Alexander, T., Genzel, R., Martins, F., Ott, T. 2009, ApJ, 692, 1075  
 Graham, A. W., & Guzmán, R. 2003, AJ, 125, 2936  
 Graham, A., & Worley, C. 2008, MNRAS, 388, 1708  
 Graham, A. W. & Spitler, L. R. 2009, MNRAS, 397, 2148  
 Graham, A. W., Driver, S. P. 2007, ApJ, 655, 77  
 Graham A. W. 2012, MNRAS, 422, 1586  
 Graham, A. W. 2012b, ApJ, 746, 113  
 Harris, W. 1996, AJ, 112, 1487  
 Hashimoto, Y., Funato, Yoko, & Makino, J. 2003, ApJ, 582, 196  
 Häring, N., & Rix, H. 2004, ApJ, 604, L89  
 Hartmann, H., Debattista, V. P., Seth, A., Cappellari, M., & Quinn, T. R., 2011, MNRAS, 418, 2697  
 Hopman, C., & Alexander, T., 2006, ApJ, L645  
 Hopkins, P. F.; Hernquist, L., Cox, T. J.; Dutta, S. N. & Rothberg, B. 2008, ApJS, 181, 486  
 Hopkins, P. F., Cox, T. J., Dutta, S. N., Hernquist, L., Kormendy, J., & Lauer, T. R. 2009, ApJS, 181, 135  
 Hughes, S. A. 2003, Annals of Physics, 303, 142  
 Inoue, S. 2009, 397, 709  
 Kruijssen, J. M. D., & Portegies Zwart, S. F. 2009, ApJ , 698, L158  
 Kruijssen, J. M. D., Pelupessy, F. I.; Lamers, H. J. G. L. M., Portegies Zwart, S. F.; Bastian, N, & Icke, V. 2012, MNRAS, 421, 1927  
 Kruijssen, 2012, (in preparation)  
 Jordán, A. et al. 2005 ApJ, 634, 1002  
 Just, A., Khan, F. M., Berczik, P., Ernst, A., & Spurzem, R. 2010, MNRAS, tnp.1687  
 Kandrup, H. E. 1990, ApJ, 364, 100  
 Kim, S. S., Morris, M. 2003, ApJ, 597, 312  
 King, I. R., 1962, AJ, 67, 471  
 King, A. 2003, ApJ, 596, L27  
 Kormendy, J. 1987, IAU, 127, 17



- Lada C. J., Lada E. A., 2003, *ARA&A*, 41, 57  
 Lamers, H. J. G. L. M., Baumgardt, H., & Gieles, M. 2010, *MNRAS*, 409, 305  
 Lauer, T. R., et al. 1992, *AJ*, 110, 2622  
 Lauer, T. R., Faber, S. M., Ajhar, E. A., Grillmair, C. J., & Scowen, P. A. 1998, *AJ*, 116, 2263  
 Lauer, T. R. et al. 2002, *AJ*, 124, 197  
 Launhardt, R., Zylka, R., & Mezger, P. G. 2002, *A&A*, 384, 112  
 Leigh, N., Böker, T., Knigge, C. arXiv  
 Loose, H. H., Kruegel, E., & Tutukov, A. 1982, *A&A*, 105, 342  
 Macchetto, F., Marconi, A., Axon, D., Capetti, A., Sparks, W., & Crane, P. 1997, *ApJ*, 489, 579  
 Matthews, L. D., & Gallagher, J. S. III 1997, *AJ*, 114, 1899  
 Matthews, L. D., et al. 1999, *AJ*, 118, 208  
 McLaughlin, D. E., King, A. R., & Nayakshin, S. 2006, *ApJ*, 650, L37  
 McMillan, P. J., & Dehnen, W. 2007, *MNRAS*, 378, 541  
 McQuillin, R. & McLaughlin, D. 2012, *MNRAS*, 423, 2162  
 Merritt, D., & Cruz, F. 2001, *ApJ*, 551, L41  
 Merritt, D., Piatek, S., Portegies Zwart, S., Hensendorf, M. 2004, *ApJ*, 608, L25  
 Merritt, D. 2009, *ApJ*, 694, 959  
 Merritt, D., 2010, *ApJ*, 718, 739  
 Merritt, D., Alexander, T., Mikkola, S., & Will, C. 2011, *PhRvD*, 84, 4024  
 Milosavljević, M. 2004, *ApJ*, 605, L13  
 Milosavljević, M. & Merritt, D. 2001, *ApJ*, 563, 34  
 Nayakshin, S., Wilkinson, M. I., King, A. 2009, *MNRAS*, 398L, 54  
 Nadeen, S. et al. 2012, arXiv1203.2625  
 Neumayer, N., & Walcher, C. J. 2012, *Adv. Astron.*, 2012, 709038  
 Oh, S., Kim, S. S., & Figer, D. F. 2009, *JKAS*, 42, 17  
 Paumard, T. 2006, *ApJ*, 643, 1011  
 Peng, E. W., 2008, *ApJ*, 681, 197  
 Preto, M., Merritt, D., Spurzem, R. 2004, *ApJ*, 613, L109  
 Pryor C., Kormendy J., 1990, *AJ*, 100, 127  
 Pfuhl, O. et al. 2011, *ApJ*, 741, 108  
 Quinlan, G. D. 1996, *New Astron.*, 1, 255  
 Read, J. I., Goerdt, T., Moore, B., Pontzen, A. P.; Stadel, J., Lake, G. 2006, *MNRAS*, 373, 1451  
 Rosenberg, A., Saviane, I., Piotto, G., & Aparicio, A. 1999 *AJ*, 118, 2306  
 Rossa, J. et al. 2006, *AJ*, 132, 1074  
 Seth A. C., Dalcanton J. J., Hodge P. W., Debattista V. P., 2006, *AJ*, 132, 2539  
 Seth, A. et al. 2008, *ApJ*, 678, 116  
 Schinnerer, E. et al. 2006, *ApJ*, 649, 181  
 Schinnerer E., Böker T., Meier D. S., & Calzetti D. 2008, *ApJL*, 684, L21  
 Scott, N., & Graham, A. W. 2012, arXiv1205.5338  
 Shlosman I., & Begelman M. C. 1989, *ApJ*, 341, 685  
 Schödel, R., Eckart, A., Alexander, T., et al. 2007, *A&A*, 469, 125  
 Schödel, R., Merritt, D., & Eckart, A. 2008, *Journal of Physics Conference Series*, 131, 012044  
 Schödel, R., Merritt, D., & Eckart 2009 *A&A*, 502, 91  
 Spitzer, L. 1987, *Dynamical evolution of Globular Clusters* (Princeton: Princeton Univ. Press)  
 Spiegel, D. N., et al. 2003, *ApJS*, 148, 175  
 Terzić, B., & Graham, A. W. 2005, *MNRAS*, 362, 197  
 Tremaine, S. D., Ostriker, J. P., & Spitzer, L., Jr. 1975, *ApJ*, 196, 407  
 Tremaine, S., & Weinberg, M. D. 1984, *MNRAS*, 209, 729  
 Trippe et al. 2008, *A&A*, 492, 419  
 Turner et al., 2012, *ApJS*, 203, 5  
 van den Bergh, S., *AJ*, 1986, 91, 271  
 Vesperini, E., 1997, *MNRAS*, 287, 915  
 Vesperini, E., 1998, *MNRAS*, 229, 1019  
 Walcher, C. J. 2005, *ApJ*, 618, 237  
 Wehner, E. H. & Harris, W. E. 2006, *ApJ*, 644, L17  
 Weinberg, M. D. 1986, *ApJ*, 300, 93  
 Yusef-Zadeh, F., Bushouse, H., & Wardle, M. 2012 *ApJ*, 744, 24  
 Young, P. J., Westphal, J. A., Kristian, J., Wilson, C. P., Landauer, F. P. 1978, *ApJ*, 221, 721